TECHNISCHE
UNIVERSITÄT
WIEN
Vienna University of Technology

DIPLOMA THESIS

LDACS-1 Airborne Receiver with High Immunity to DME Systems

supervised by

Ass.Prof. Dipl.-Ing. Dr.techn. Holger Arthaber
and
O.Univ.Prof. Dipl.-Ing. Dr.techn. Gottfried Magerl

performed at the
Institute of Electrodymamics, Microwave and Circuit Engineering

by

Reinhard Koeppner, BSc.
Matr.Nr. 0425153
Kaiser-Ebersdorfer-Straße 35/1/26, 1110 Wien

Vienna, October 2012

DIPLOMARBEIT

LDACS-1 Airborne Receiver with High Immunity to DME Systems

ausgeführt zum Zwecke der Erlangung des akademischen Grades
eines Diplom-Ingenieurs

unter der Leitung von

Ass.Prof. Dipl.-Ing. Dr.techn. Holger Arthaber
und
O.Univ.Prof. Dipl.-Ing. Dr.techn. Gottfried Magerl

Institute of Electrodymamics, Microwave and Circuit Engineering

eingereicht an der Technischen Universität Wien
Fakultät für Elektrotechnik und Informationstechnik

von

Reinhard Koeppner, BSc.
Matr.Nr. 0425153
Kaiser-Ebersdorfer-Straße 35/1/26, 1110 Wien

Wien, im Oktober 2012

Abstract

Air-traffic is rapidly increasing and is expected to have nearly doubled in Europe in 2030 compared to nowadays. As capacities are limited with the actual structure of air-traffic management, a new way needs to be found which, additionally, provides even higher security standards. The European Commission founded project '*SESAR*' aims at achieving this target by the concept of trajectory based (instead of 'waypoint-to-waypoint') routing: Each aircraft shall get its preferred route and time of arrival. One major part in this concept is LDACS-1: A highly reliable wireless data link between aircraft and ground as well as between aircrafts.

The goal of this diploma thesis is the design of an LDACS-1 compliant receiver prototype. It operates in L-band at $960 \ldots 1164\,\mathrm{MHz}$ with a $0.5\,\mathrm{MHz}$ channel bandwidth. The receiver has to handle input signal power levels of $-104 \ldots -10\,\mathrm{dBm}$ and must withstand high interference power up to $25\,\mathrm{dBm}$ introduced by the DME navigation system. Thus, the major challenge for the design is the combination of high sensitivity and linearity while maintaining immunity against strong interferers.

In this work the complete RF frontend for an LDACS-1 receiver is designed and measured. The development starts with the choice of the receiver structure and considerations regarding noise figure and linearity, continuing with the component selection and the simulation of the whole receiver chain. As some components lack implementation critical specifications, appropriate methods are found to measure and verify them. Thereafter, a custom designed PCB containing the complete receiver chain is presented. Measurements show that the presented prototype fulfills and even surpasses the LDACS-1 requirements.

Kurzfassung

Das Luftverkehrsaufkommen steigt rasant und wird sich bis zum Jahr 2030 im Vergleich zu heute nahezu verdoppelt haben. Da die derzeitigen Managementstrukturen für den Flugverkehr ihre Kapazitätsgrenzen haben, muss eine neue Organisationsmethode gefunden werden, die nicht nur die Kapazität, sondern gleichzeitig auch die Sicherheit erhöht. Das durch die Europäische Kommission gegründete Projekt '*SESAR*' soll dieses Ziel durch eine direkte Streckenführung (statt der derzeitigen 'Wegpunkt-zu-Wegpunkt'-Strategie) erreichen. Jedes Flugzeug soll dabei seine eigene optimale Strecke und Ankunftszeit bekommen. Ein wichtiger Teil dieses Projektes ist LDACS-1: eine hochzuverlässige drahtlose Datenverbindung sowohl zwischen Flugzeugen und Bodenstationen, als auch zwischen den Flugzeugen selbst.

Das Ziel dieser Diplomarbeit ist die Entwicklung eines LDACS-1 konformen Empfänger-Prototypen. Dieser arbeitet im L-Band von $960 \ldots 1164\,\mathrm{MHz}$ mit einer Bandbreite von $500\,\mathrm{kHz}$. Der Empfänger muss Signalpegel von $-104 \ldots -10\,\mathrm{dBm}$ verarbeiten und den, durch das DME-Navigationssystem verursachten, Störleistungen von bis zu $25\,\mathrm{dBm}$ standhalten. Daraus ergibt sich die Herausforderung eine hohe Empfindlichkeit und Linearität mit der Unempfindlichkeit gegenüber starken Störern zu kombinieren.

Diese Arbeit zeigt das Design und die Messung eines kompletten HF-Frontends für einen LDACS-1 Empfänger. Die Entwicklung beginnt mit der Wahl der Empfängerstruktur und Überlegungen zu Rauschzahl und Linearität, gefolgt von der Bauteilauswahl und der Simulation der ganzen Empfangskette. Für einige Komponenten existieren unspezifierte Parameter, welche für die Implementierung kritisch sind. Daher werden geeignete Methoden gefunden, um diese zu messen und zu verifizieren. Danach wird eine eigens entworfene Leiterplatte präsentiert, welche die ganze Empfängerkette beinhaltet. Die Messungen zeigen, dass der hier vorgestellte Prototyp die LDACS-1 Anforderungen erfüllt und sogar übertrifft.

To my parents.

Contents

1 Introduction **1**
- 1.1 Motivation . . . 1
- 1.2 Single European Sky . . . 2
- 1.3 Aeronautical Communication Systems . . . 4
  - 1.3.1 LDACS: The Future Continental Aeronautical Communication System . . . 5
  - 1.3.2 LDACS-1 Prototype . . . 6

2 Derivation of the LDACS-1 Receiver Requirements **7**
- 2.1 System Description . . . 7
  - 2.1.1 Deployment Options . . . 8
- 2.2 Signal Path Scenarios . . . 9
  - 2.2.1 Path Loss . . . 9
  - 2.2.2 Scenarios . . . 10
- 2.3 Interference Scenarios . . . 11
  - 2.3.1 Existing Systems . . . 11
  - 2.3.2 DME System . . . 13
- 2.4 Receiver Requirements . . . 15
  - 2.4.1 SNR . . . 15
  - 2.4.2 Noise Figure . . . 17
  - 2.4.3 Resulting Receive Power . . . 17
  - 2.4.4 Gain Range Requirements for ADC Interfacing . . . 17
  - 2.4.5 Absolute Maximum Input Power . . . 19
  - 2.4.6 Input 1 dB compression point P1dB . . . 19
- 2.5 Summary . . . 19

3 Receiver Design **20**
- 3.1 Receiver Structure Selection . . . 20
  - 3.1.1 Homodyne vs. Heterodyne Receiver . . . 20
  - 3.1.2 Noise Figure Considerations . . . 25
  - 3.1.3 Conclusion . . . 26

3.2 Component Selection . . . 26
3.2.1 Band Selection Filter . . . 27
3.2.2 Low Noise Amplifier . . . 27
3.2.3 Mixer . . . 28
3.2.4 IF Filter . . . 29
3.2.5 Variable Gain Amplifier . . . 31
3.2.6 IF Gain Stage . . . 35
3.3 Performance Analysis of the Receiver . . . 35
3.3.1 Noise Figure . . . 36
3.3.2 Gain Range . . . 36
3.3.3 Input 1 dB Compression Point (P1dB) . . . 36
3.3.4 Absolute Maximum Input Power . . . 38
3.3.5 Link Budget . . . 43
3.4 Summary . . . 44

4 Receiver Chain Measurements 45
4.1 Verification measurements . . . 47
4.1.1 Gain . . . 47
4.1.2 P1dB . . . 49
4.1.3 Noise Figure . . . 49
4.1.4 Recovery Time . . . 51
4.1.5 Frequency Response . . . 54
4.1.6 Signal to Noise Ratio . . . 54
4.2 Summary . . . 58

5 Summary and Outlook 59
5.1 Summary . . . 59
5.2 Outlook . . . 59

Appendices 63

A Noise Figure Calculation 64

Abbreviations

A/A	...	Air-to-Air
A/G	...	Air-to-Ground
ACARS	...	Aircraft Communications Addressing and Reporting System
ADC	...	Analog to Digital Converter
ADS-B	...	Automatic Dependent Surveillance - Broadcast
AGC	...	Automatic Gain Control
AS	...	Aircraft Station
ATC	...	Air Traffic Control
ATM	...	Air Traffic Management
ATT	...	Attenuator
BB	...	BaseBand
BBA	...	BaseBand Amplifier
BER	...	Bit Error Rate
BP	...	Bandpass
COM	...	Communication
CW	...	Continuous Wave
DAC	...	Digital to Analogue Converter
DC	...	Direct Current
DME	...	Distance Measuring Equipment
DUT	...	Device Under Test
EIRP	...	Equivalent Isotropically Radiated Power
ENR	...	Excess Noise Ratio
FCI	...	Future Communication Infrastructure
FEC	...	Forward Error Correction
FFT	...	Fast Fourier Transformation
FL	...	Forward Link
FPGA	...	Field Programmable Gate Array
FSPL	...	Free Space Path Loss
FWHM	...	Full Width Half Maximum
G/G	...	Ground-to-Ground
GMSK	...	Gaussian Minimum Shift Keying

GNSS	...	Global Navigation Satellite System
GPS	...	Global Positioning System
GS	...	Ground Station
GSM	...	Global System for Mobile Communications
HD	...	Harmonic Distortion
ICAO	...	International Civil Aviation Organization
IF	...	Intermediate Frequency
IIR	...	Infinite Impulse Response
IF	...	Intermediate Frequency
IL	...	Insertion Loss
IMD	...	Intermodulation Distortion
IMP	...	Intermodulation Products
I	...	In-phase
JTIDS	...	Joint Tactical Information Distribution System
LDACS	...	L-band Digital Aeronautical Communications System
LO	...	Local Oscillator
LNA	...	Low Noise Amplifier
MEO	...	Medium Earth Orbit
MSPS	...	Million Samples Per Second
NF	...	Noise Figure
OFDM	...	Orthogonal Frequency Division Multiplex
P1dB	...	1 dB Compression Point
PA	...	Power Amplifier
PAPR	...	Peak to Average Power Ratio
PCB	...	Printed Circuit Board
Q	...	Quadrature
QAM	...	Quadrature Amplitude Modulation
RADAR	...	Radio Detection and Ranging
RBW	...	Resolution BandWidth
RL	...	Reverse Link
RF	...	Radio Frequency
RX	...	Receiver
SA	...	Spectrum Analyzer
SATCOM	...	SATellite COMmunication
SAW	...	Surface Acoustic Wave
SESAR	...	Single European Sky ATM Research
SNR	...	Signal to Noise Ratio
SSR	...	Secondary Surveillance Radar
UAT	...	Universal Access Transceiver
VGA	...	Variable Gain Amplifier
VHF	...	Very High Frequency (30 . . . 300 MHz)

Chapter 1

Introduction

1.1 Motivation

The first controlled and powered human flight was performed by the *Wright Brothers* in 1903. As at this time there was no other air traffic, there was no need for any kind of regulation and organization of the airspace.
The development of aviation started progressing rapidly and soon there was the need to coordinate the increasing number of aircrafts. The first worldwide half-duplex Very High Frequency (VHF) voice communication system has been established by the International Civil Aviation Organization (ICAO), a sub-agency of the United Nations that has been founded at the 'Chicago convention' in 1944.
Modern Air Traffic Management (ATM) still relies on the VHF system for the communication between the control center and the pilot. In addition to that, usually a 'Radio Detection And Ranging' (RADAR) localization system is used which gives the controller an overview of all aircraft's position in his area of responsibility. Based on this information a safe guidance of all planes within the airspace can be provided.

Air-traffic is still increasing and is expected to have nearly doubled in Europe in 2030 compared to nowadays[1]. As capacities are limited with the actual structure of air-traffic management, there has to be a more efficient way, while providing even higher security standards. The key points for reaching these targets will be a standardization of ATM and a simplified airspace structure which is presently very fragmented due to territorial regulations and political frontiers.

The European Commission founded project 'Single European Sky ATM Research' (*SESAR*) aims at achieving this target by the concept of trajectory based (instead of 'waypoint-to-waypoint') routing: Each aircraft shall get its preferred route and time of arrival. As a basis for this system with the so called '4D trajectories', a reliable data link between aircraft and ground (later shortly termed as A/G) and also aircraft to aircraft (A/A) is needed. Existing data link systems were intended for transmission of short and simple text messages (usually 100 to 200 characters) and will not be able to cover future requirements. A multi-link concept was derived by the *SESAR* project which intends to combine existing and future systems. One major part in this concept is LDACS (L-band Digital Aeronautical Communication System). As the name implies, this communication system will operate in the L-band which is spectrally located around 1 GHz. Since this band is already crowded mainly by navigation systems, LDACS will have to deal with all existing systems and vice versa.
Due to the requirement that communication shall be possible over a wide range of distances—dozens of meters at the airport, up to 200 nautical miles at the cell boundaries—the system will have to show a high dynamic range. In combination with the spectrally nearby located interferers, this is quite challenging for the RF frontend.

In this thesis, a prototype of such an RF frontend shall be developed and characterized, which allows performance verifications and compatibility tests against existing in-band systems and important 'spectral neighbors' like GPS and GSM.

1.2 Single European Sky

The current ATM system was developed mainly in the first half of the twentieth century. It relies on aircraft routing based on waypoints like radio beacons. The direction an aircraft flies is only changed at this waypoints so that the resulting way flown is a kind of a zig-zag. Additionally, there are slightly different regulations in each country which lead to different routing standards like the flying altitude when crossing borders. This causes unnecessary climbs and descends during a flight. It is obvious that this will not be the optimal route between departure and arrival airport.
The airspace overhead Europe has become more and more fragmented and sectorized during the last decades. The main reason for this comes from the fact that one human controller can only serve a maximum amount of traffic at the same time, which means that for growing traffic the ATM structure would require even more slicing. For finer and finer partitioning the required

coordination complexity increases rapidly so that this technique leads to an capacity bound which has nearly been reached already. As a consequence, more and more flights would be delayed if the ATM remains in the present structure. Figure 1.1 illustrates the basic airspace fragmentation of Austria in 2011, not showing that this basic structure is again sectorized in the vicinity of airports.

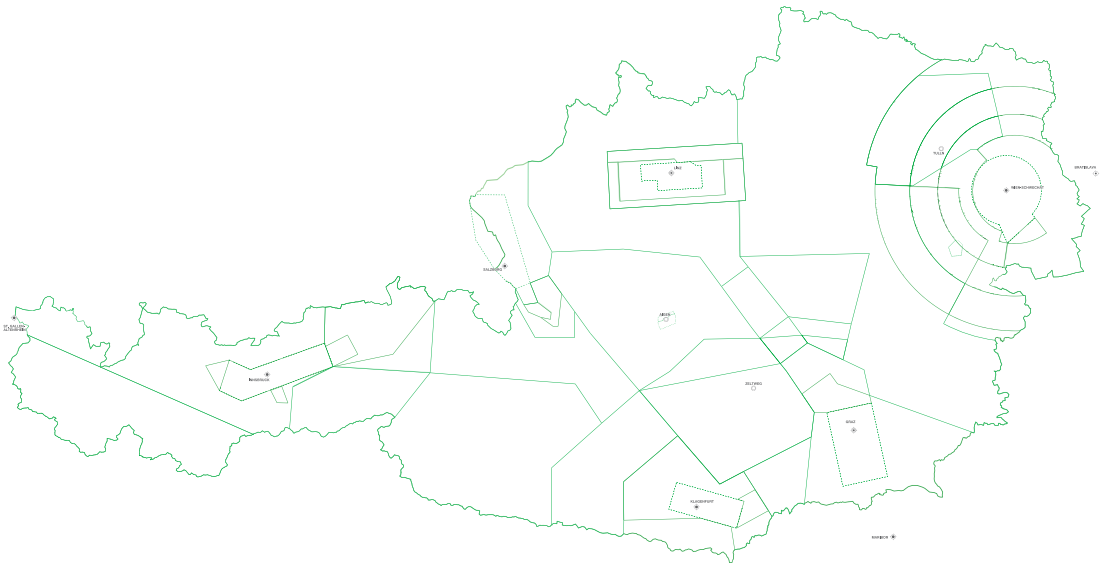

Figure 1.1: Exemplary basic airspace structure of Austria in 2012 [2].

This way of organization also includes a security issue since all aircrafts use the same virtual waypoints for their routing which leads to a spatial concentration there. The risk that they could collide there is quite evident and still increasing with additional air traffic.

So, one aim of the SESAR project is to increase separation of air-traffic by removing the need for fixed waypoints but use the former mentioned '*4D trajectories*' so that every aircraft is getting its specific route. The resulting European airspace is then divided only in a few parts called 'Functional Airspace Blocks' instead of dozens of national airspaces. This new concept is expected to simultaneously increase security and capacity while adding efficiency (reduced fuel consumption).

1.3 Aeronautical Communication Systems

Future aeronautical communication systems for a single European sky shall rely on the SESAR Future Communication Infrastructure (FCI) which is a multi-link concept. It is divided into legacy systems (such as existing VHF voice communication systems), airport surface, general terrestrial, and satellite communication systems. Figure 1.2 illustrates how these systems are planned to interact. Air-to-ground and air-to-air communications are termed as A/G and A/A, respectively.

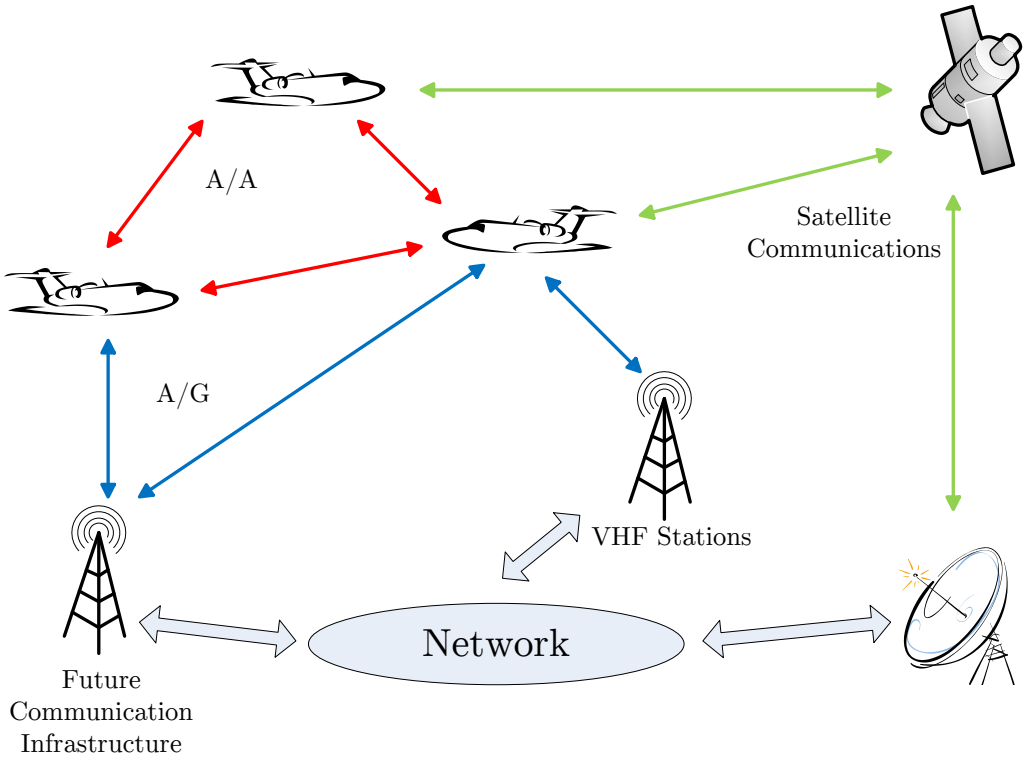

Figure 1.2: Interaction of aeronautical communication systems.

Nowadays, the complete ATM relies on the VHF voice communication system. Future communication systems will require the exchange and coordination of the 4D trajectories of each flight so there has to be an additional data link. It will be the key technology for modern ATM and, therefore, has to show high reliability. For this reason the SESAR FCI is based onto four main technologies for different communication types and areas of coverage (acting as backup for each other if one fails):

- Legacy systems such as the VHF voice communication system will still be used as an important link between controller and pilot

- L-band communications—namely LDACS—will be used for general continental data links
- C-band communications (around 5.8 GHz) are planned for high traffic areas like airports
- Satellite systems will be used where the other technologies have no coverage (e.g. oceanic regions)

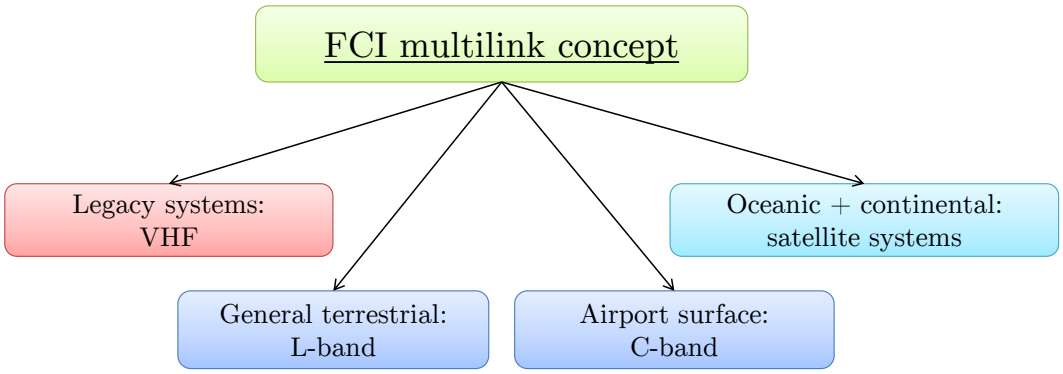

Figure 1.3: SESAR FCI multi-link concept.

1.3.1 LDACS: The Future Continental Aeronautical Communication System

The SESAR project foresees two deployment options for digital communication: A Frequency Division Duplex (FDD) with an OFDM modulation and the other using a Time Domain Duplex (TDD) utilizing GMSK modulation. In a first step a prototype demonstrator for the favored FDD option (**LDACS-1**) shall be built. The TDD option (**LDACS-2**) would only be evaluated if the specified requirements cannot be fulfilled by LDACS-1 in laboratory tests.

1.3.2 LDACS-1 Prototype

As part of a cooperation of the *Institute of Electrodynamics, Microwave and Circuit Engineering (EMCE)* from *Vienna University of Technology* and the *Frequentis AG* (in what follows shortly termed *Frequentis*) an LDACS-1 transceiver prototype shall be developed.
The development is divided and organized as follows:

- Baseband unit (including ADC/DAC interfacing): by *Frequentis*
- RF part: by *EMCE* in the context of three diploma theses covering:
  - Receiver
  - Transmitter
  - Reference receiver for accomplishing transmitter linearization

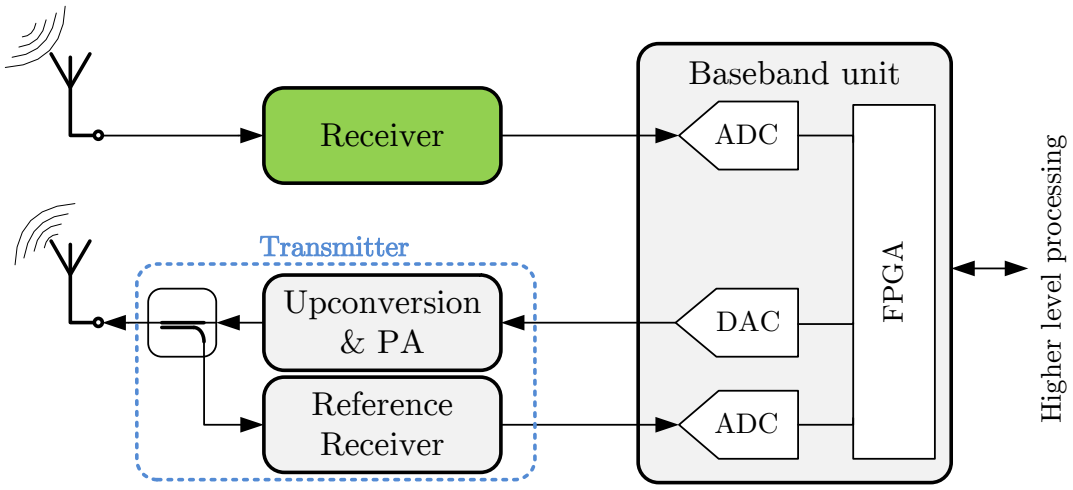

Figure 1.4: Organizational structure of the LDACS-1 transceiver prototype.

This thesis is intended to present the development of receiver prototype (Figure 1.4).

Chapter 2

Derivation of the LDACS-1 Receiver Requirements

First a short general system description of LDACS-1 shall be given, continuing with the requirements regarding the compatibility with existing legacy systems. By investigating signal path, interference scenarios, and other limitations the requirements for the RX prototype will be derived.
The prototype design itself will be presented in Chapter 3.

2.1 System Description

LDACS-1 operates in the L-band at 960...1164 MHz. It is designed as a cellular communication system with seamless and automatic handover between cells enabling future aeronautical data links with data rates of 300...1300 kbits/s. There will also be an optional support for digital voice links which could replace nowadays analogue VHF voice links.
As the L-band is already crowded by a bunch of existing aeronautical as well as military systems, it is designed as a so called inlay system not requiring the allocation of an own free spectrum. Instead, it was designed to 'lay' into spectral gaps of existing systems which inevitably results in mutual interference problems. As some of the existing systems have quite relaxed spectral specifications (from a modern communication system point of view) and can neither be modified nor may be disturbed, the LDACS-1 has to take most of the load. This fact creates the need for a stringent spectral mask for the LDACS-1 transmitter and the handling of strong interference for the receiver.
As described in Section 2.3, the *Distance Measuring Equipment* (DME) navigation system is the major user of the L-band. Since it operates in FDD mode with

a 1 MHz channel spacing, LDACS-1 was designed with a 0.5 MHz channel grid which offers a maximum of flexibility and a direct inlay ability into the spectral gaps of DME.
According to [3] the A/A mode was out of scope in the LDACS study, therefore only the parameters for A/G mode were specified in detail. Although the two modes differ in physical and data link layer parameters, both utilize FDD with OFDM modulation. The main physical layer parameters are summarized in Table 2.1.

Number of total subcarriers	N_{FFT}	64
Number of used subcarriers	N_u	50
Total FFT bandwidth	B_0	625.0 kHz
Occupied RF bandwidth	B_{occ}	498.05 kHz
Subcarrier spacing	Δf	9.765625 kHz
Useful OFDM symbol time	T_s	102.4 μs

Table 2.1: LDACS-1 main physical layer parameters.

2.1.1 Deployment Options

The LDACS-1 system specification foresees two basic options for spectral deployment with the possibility of a combination of both:

- Inlay deployment utilizing two 24 MHz bands (985...1009 MHz and 1048...1072 MHz with a channel grid of 1 MHz) in a DME occupied frequency range. This option is proposed for initial prototyping.
- Non-inlay deployment utilizing two 7 MHz bands (963.5...970.5 MHz and 1149.5...1156.5 MHz with a channel grid of 0.5 MHz) in non-occupied parts of the L-band. This is an alternative deployment proposal.

The Forward Link (FL) defines the link between Ground Station (GS) and airborne station (AS) and the Reverse Link (RL) vice versa. Their spectral position is not fixed yet for the second deployment option and may be swapped (Figure 2.1). This is of minor importance in this thesis since the design of the receiver for the GS and AS will be the same due to very similar requirements.
The frequency duplex spacing between FL and RL is 63 MHz for the inlay option (which is actually again the same as for the DME system) or 186 MHz for the non-inlay option, respectively.

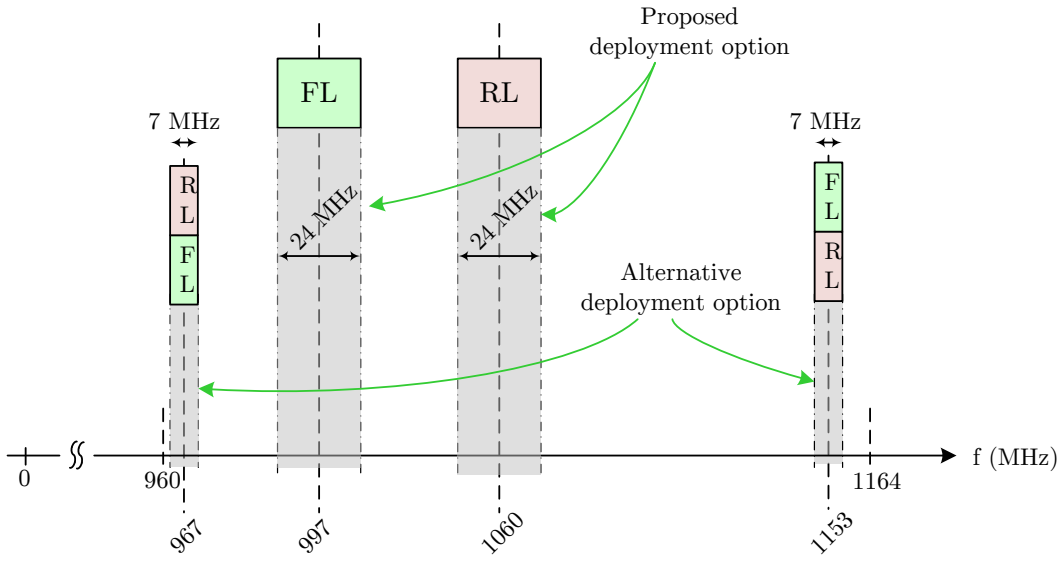

Figure 2.1: Deployment options of LDACS-1.

2.2 Signal Path Scenarios

In this section the expected signal path loss in different possible scenarios is shown. This serves as the basis for Section 2.4 where the concrete RF requirement parameters for the receiver prototype are worked out.

2.2.1 Path Loss

There are various effects on propagating waves that contribute when calculating the path loss between two devices. The simple case of free space path loss (FSPL) can be assumed, if two conditions are fulfilled:

- The path is clear of obstacles in the first *Fresnel* zone.
- The distance between the antennas must be greater than the *Rayleigh* distance $r_R = \frac{2D^2}{\lambda}$ which is $\approx$34 cm here[1] (assuming a quarter wavelength dipole antenna with $D = \lambda/4 = 7.5\,\text{cm}$). This will even be the case if two such antennas are mounted on the same aircraft (opposite sides of the fuselage).

In [4] the FSPL is used as an approximation although the first condition is probably not fulfilled for some scenarios (e.g. aircraft on the ground communicating

[1] D is the size of the antenna in meters. A frequency of 1 GHz was assumed.

with a ground station). So, the path loss for the scenarios in the following sections will be calculated using Equation 2.1 where d is the distance in meters.

$$\mathrm{FSPL} = \left(\frac{4\pi d}{\lambda}\right)^2 \qquad or \qquad \mathrm{FSPL_{dB}} = 20\log_{10}\left(\frac{4\pi d}{\lambda}\right). \tag{2.1}$$

2.2.2 Scenarios

There are 12 different scenarios proposed in [4]. Since some of them are coincident or not relevant for the considerations regarding the receiver requirements, it is only dealt with the four cases illustrated in Figure 2.2.

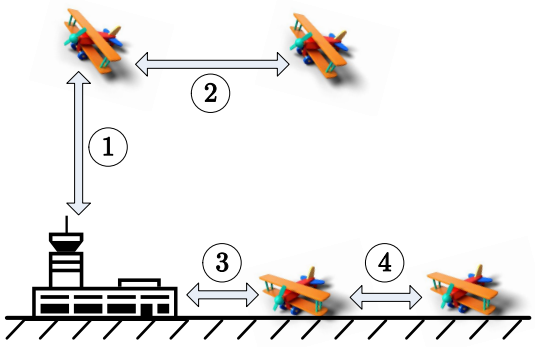

Figure 2.2: Signal path scenarios.

1. A/G: AS airborne ↔ GS
   This scenario covers the link between an airborne aircraft and a ground station. The minimum distance, and so the minimum path loss, is 50 m which will usually occur in the take-off/landing phase of the aircraft when it passes the GS antennas which are possibly mounted in the proximity of the runway. The maximum distance will be observed when the AS is at the extremities of the operational range of LDACS-1 which is 200 nautical miles (370.4 km).

2. A/A: AS airborne ↔ AS airborne
   The minimum separation between airborne aircrafts is 1000 ft, corresponding to ≈305 m. The maximal distance will be, like in the first scenario, 200 NM as this is the maximal operational range of LDACS-1 .

3. G/G: GS ↔ GS
   This scenario applies for the communication between an AS on ground to a GS. The distance depends on the parking positions and can vary between 50 m and 2.5 km at large airports.

4. G/G: AS on ground ↔ GS As the same distances as in Scenario 3 are assumed this scenario is equivalent to it.

Scenario	$\mathbf{d_{min}}$**(m)**	$\mathbf{d_{max}}$**(km)**	$\mathbf{FSPL_{min}}$**(dB)**	$\mathbf{FSPL_{max}}$**(dB)**
1	50	370.4	66	144
2	305	370.4	82	144
3	50	2.5	66	100

Table 2.2: Distance and FSPL of main signal path scenarios.

So, if these scenarios are condensed, the link distance varies from 50 m to 370.4 km, corresponding to path losses of 66...144 dB. The detailed minimal/maximal path losses are summarized in Table 2.2.

2.3 Interference Scenarios

In the last section the attenuation on the LDACS-1 link was investigated. As shortly mentioned in Section 2.1, there are legacy systems existing in or near the L-band. The influences of them onto the LDACS-1 receiver shall be investigated now. The reversed consideration is neglected here since the receiver is not expected to have a significant radiation (this would apply to the LDACS-1 transmitter only which is out of scope of this thesis).

2.3.1 Existing Systems

This section first investigates the spectral surroundings of the L-band (to see if there are possible interfering systems from 'outside') and continues with the existing in-band systems.

2.3.1.1 Out-of-Band Systems

As illustrated in Figure 2.3 the two major spectral neighbors of the L-band are GSM900 and GNSS:

- *Global Navigation Satellite System* (GNSS)
  There are a couple of GNSS systems like GPS (US), GLONASS (Russia), COMPASS (China), and Galileo (EU) using satellites at Medium Earth Orbits (MEO) for global navigation purposes[2]. These systems operate in

[2]Flying in a altitude of about 20,000 km.

the frequency range around $\approx 1200 \ldots 1500$ MHz. As the equipment installed at AS or GS have no need for an uplink to the satellites, they are not transmitting anything. The limited transmission power of the satellites results in very low power received by an LDACS-1 receiver. Since the RX band selection filter introduces additional attenuation the influence of these GNSS systems on the receiver can be neglected.

- *Global System for Mobile Communications* (GSM)
  As stated in [4] there is an EIRP limit of 62 dBm for this band. The spectral mask for GSM base stations foresees -80 dBc attenuation for an offset from the carrier of $\geq$6 MHz. In the worst case this gives a maximum power of -100 dBm at the input of the LDACS-1 receiver (assuming 66 dB path loss as at Scenario 3 in Section 2.2.2 and further 16 dB attenuation of the band selection filter as proposed in [4]).

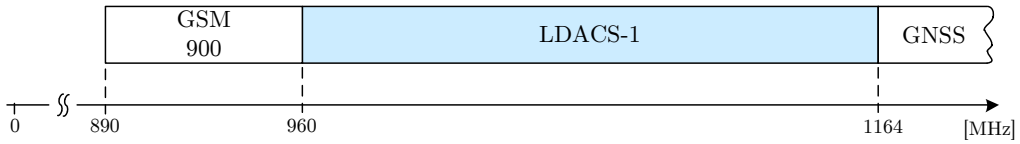

Figure 2.3: Spectral neighbors of LDACS-1 .

2.3.1.2 In-Band Systems

As shown in the previous section spectral neighbors will not bother when designing the receiver. As denoted before this will not be the case for in-band systems. A look on them identifies possible interferers:

- Secondary Surveillance Radar (SSR)
  Is a radar system for ATC purposes which uses interrogating pulses at 1030 MHz sent by a ground station. The aircraft equipment (called 'transponder') replies on 1090 MHz containing information like aircraft identification, altitude, or position.

- Universal Access Transceiver (UAT)
  Is a data broadcast service for the ADS-B surveillance system and operates at a fixed frequency of 978 MHz.

- Joint Tactical Information Distribution System (JTIDS)
  Is a frequency hopping system (51 carrier frequencies, 3 MHz spacing) mainly used by NATO for air and missile defense communications. It operates at three bands (969 . . . 1008 MHz, 1053 . . . 1065 MHz, and 1113 . . . 1206 MHz), overlapping the LDACS-1 frequencies.

- Distance Measuring Equipment (DME)
  Is a system for radio navigation working like a 'reversed' SSR. It measures the distance to a known station on the ground by determining the round triptime. This will be the most interfering system for the LDACS-1 receiver.

Table 2.3 gives a overview about the maximal interference power levels at the LDACS-1 receiver [4]. Since these are worst case scenario assumptions, interference will typically be less severe.

System	**EIRP(dBm)**	$\mathbf{P_{Interferer_{ANT}}(dBm)}$ (received by antenna)	$\mathbf{P_{Interferer_{RXmax}}(dBm)}$ (after bandpass filter)
SSR	62	36	−9
UAT	54	−15	−40
JTIDS	57	−9	−9
DME	58.5	23.5	**23.5**

Table 2.3: In-band interferer power.

Since the power of the DME system is higher by a factor of ≈30 dB after the bandpass filter [3] the other systems can be neglected for further interference considerations [5].

2.3.2 DME System

The DME system is the interfering system with the largest power level (Section 2.3.1.2) and, therefore, deserves closer attention to get an impression of the nature of interference. DME is used for radio navigation purposes and utilizes short Gaussian shaped pulses with high power levels for achieving the desired range and accuracy requirements. The system operates in the frequency range of 962. . . 1263 MHz, covering most of the aeronautical L-band. It is a FDD system utilizing 126 channels with a channel spacing of 1 MHz and a duplex distance of 63 MHz.
Figure 2.4 shows the envelope of a typical DME pulse pair that can be represented in the passband (PB) as in Equation 2.2b using a Gaussian shaped baseband pulse $d_{BB}(t)$ (Eq. 2.2a) on the DME carrier frequency [5].

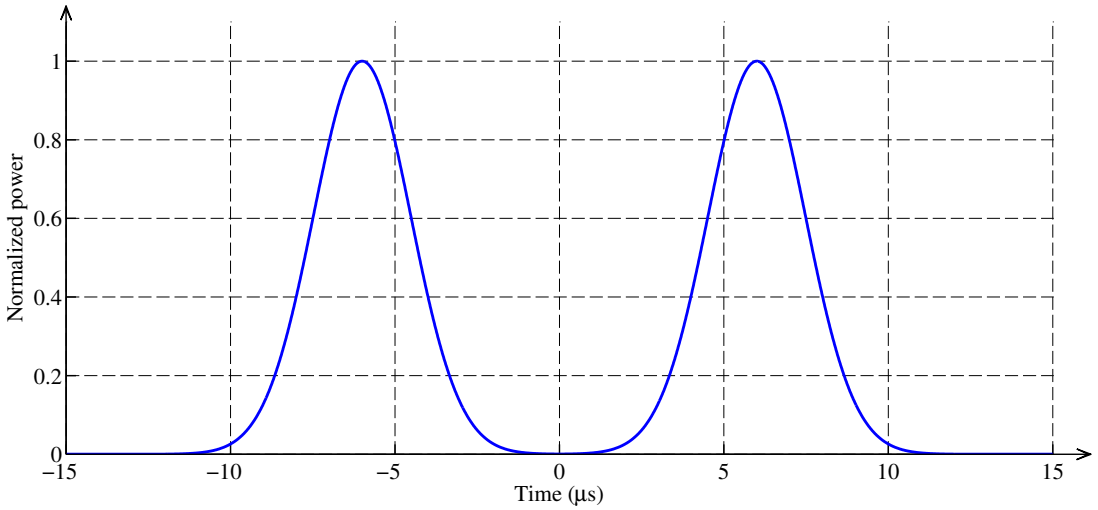

Figure 2.4: Typical DME pulse pair RF envelope $|d_{PB}(t)|$. The pulses are spaced Δt =12 μs, each with a pulse width of $FWHM_{Pulse}$ =3.5 μs.

$$d_{\mathrm{BB}}(t) = e^{-\frac{\alpha \cdot t^2}{2}} \tag{2.2a}$$

$$d_{\mathrm{PB}}(t) \propto \left[d_{\mathrm{BB}}(t + \frac{\Delta t}{2}) + d_{\mathrm{BB}}(t - \frac{\Delta t}{2}) \right] \cdot e^{j2\pi f_c t} \tag{2.2b}$$

A single Gaussian shaped pulse leads to a Gaussian shaped spectrum too (Eqn. 2.3). Since DME pulses are arranged pair-wise, the Gaussian spectrum gets 'modulated' by a cosine function as derived in Eq. 2.4. Figure 2.5 illustrates the theoretical spectrum of four adjacent DME channels and also indicates the location of one possible LDACS-1 channel in the inlay configuration (see Section 2.1.1).

$$d_{\mathrm{BB}}(t) \circ\!\!-\!\!\bullet\, G_{\mathrm{BB}}(f) = \mathcal{F}\left[d_{\mathrm{BB}}(t)\right](f) = \sqrt{\frac{2\pi}{\alpha}} \cdot e^{-\frac{2\pi^2}{\alpha} f^2} \tag{2.3}$$

$$\begin{aligned} G_{\mathrm{PB}}(f) &= G_{\mathrm{BB}}(f - f_c) \cdot \left[e^{-\jmath\pi(f-f_c)\Delta t} + e^{\jmath\pi(f-f_c)\Delta t} \right] \\ &\propto G_{\mathrm{BB}}(f - f_c) \cdot \cos\left[\pi\,(f - f_c)\,\Delta t\right] \end{aligned} \tag{2.4}$$

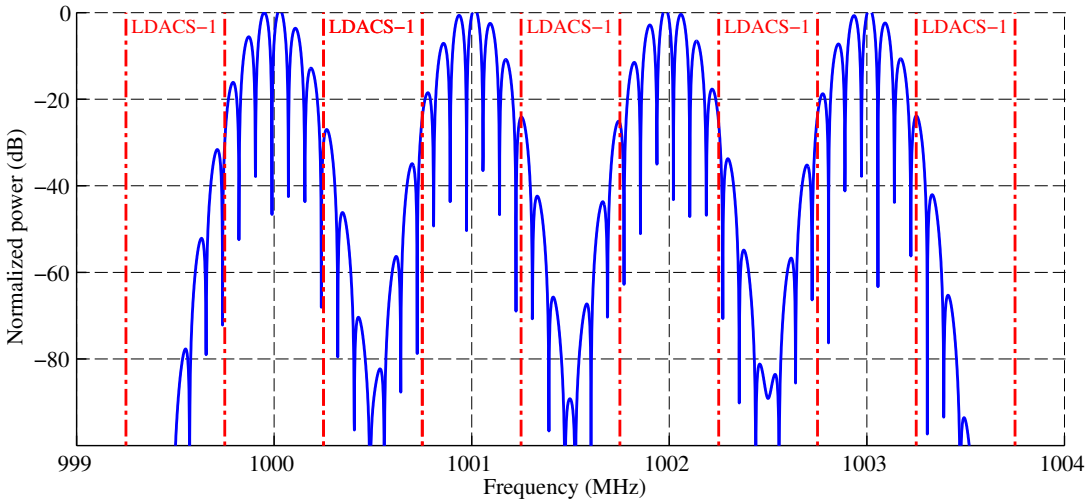

Figure 2.5: Spectrum of four adjacent DME channels. Possible LDACS-1 channels are located in the spectral gaps when operating in inlay mode.

2.4 Receiver Requirements

This section presents the requirements for the receiver. Two essential parameters for the receiver design, namely Signal to Noise Ratio (SNR) and gain range, are not directly specified in the LDACS-1 standard but are derived out of other specifications.

2.4.1 SNR

The major requirement for the complete receiver which includes RF frontend and the baseband processing, is a bit error rate BER $\leq 10^{-6}$ at the minimal specified signal input power of $-104\,\mathrm{dBm}$ (Sec. 2.4.3). The BER cannot be determined directly as it would require the complete baseband unit which is not available in the prototyping phase. Therefore, it is necessary to 'convert' the targeted BER to an appropriate RF requirement which allows the verification of the frontend presented in this thesis. Since the major factor influencing the BER is the SNR, a required minimum value for the SNR has to be derived.
In the LDACS-1 communication system a concatenation of Reed-Solomon and convolutional channel coding followed by an interleaver [6] is used for *Forward Error Correction* (FEC). To determine the minimum SNR level, a *Monte Carlo* simulation of the system is performed as shown in Figure 2.6. Figure 2.7 shows the resulting BER over SNR diagram of the system, showing that $\mathbf{SNR_{min} \approx 4.7\,dB}$.

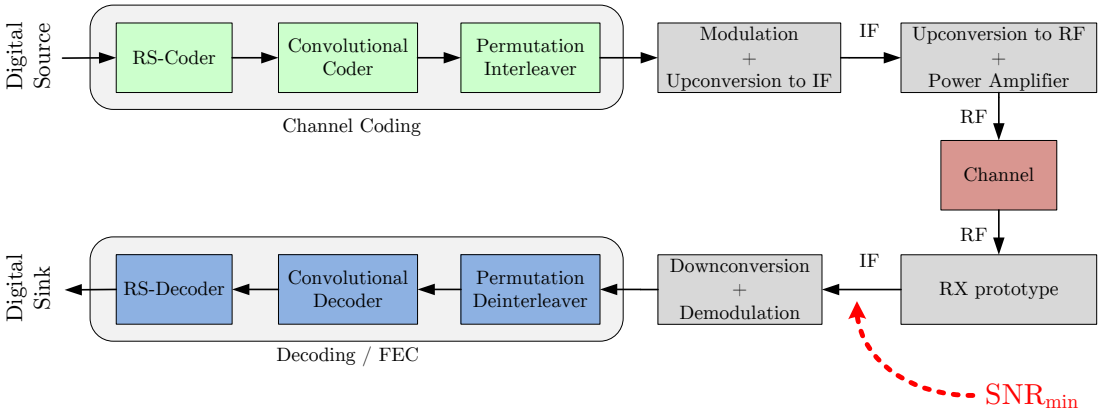

Figure 2.6: Block-diagram of channel coding and interleaving.

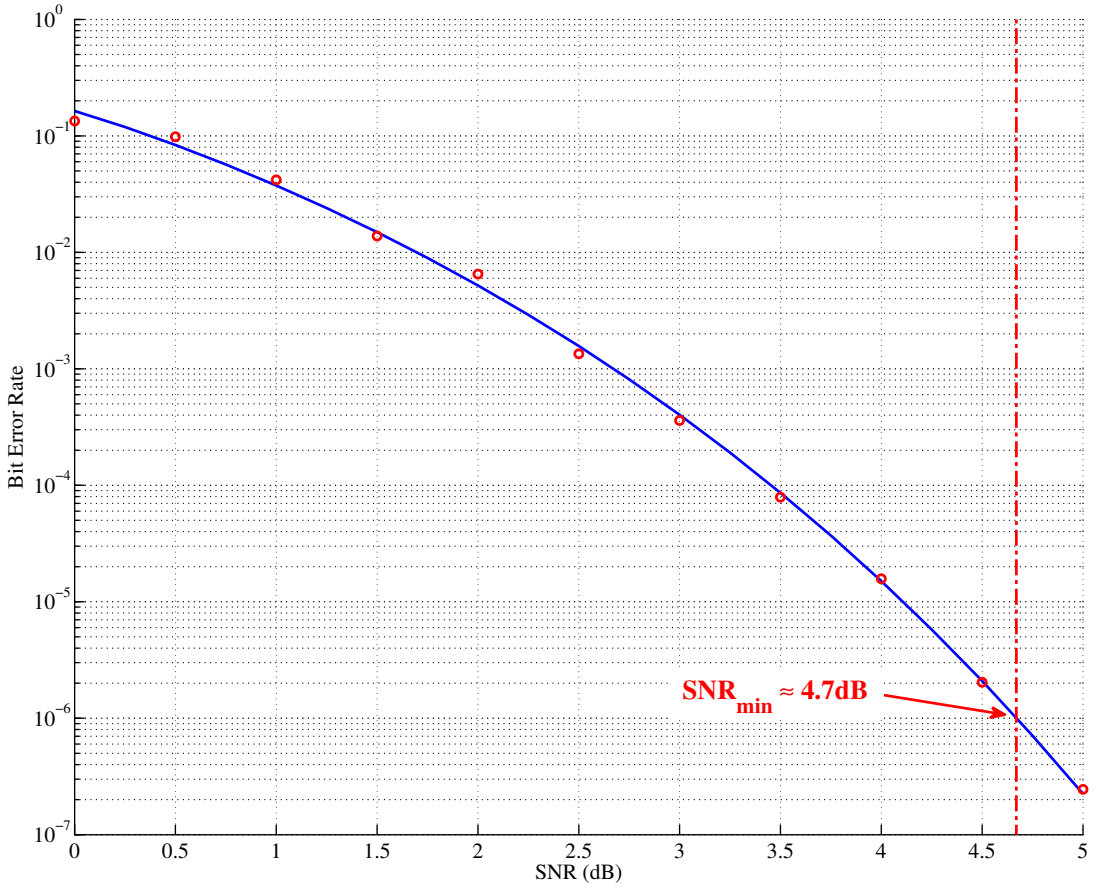

Figure 2.7: LDACS-1 Bit Error Rate plotted over the required SNR at the RF frontend output / demodulator input.

2.4.2 Noise Figure

As one of the major RF performance parameters, the noise figure (NF) of the RF frontend is specified [6] to be $\mathbf{F_{RX_{total}}} \leq \mathbf{5\,dB}$ at the receiver input (not including band filter, duplexer, and cable insertion losses).

2.4.3 Resulting Receive Power

The minimum sensitivity level for the receiver, as specified in [3], is $\mathbf{P_{RX_{min}}} = \mathbf{-104\,dBm}$ (−93 dBm peak). As stated in Section 2.4.1, the BER after FEC is specified to be less than 10^{-6} at this level. The receiver also shall be capable of decoding signals with $\mathbf{P_{RX_{max}}} = \mathbf{-10\,dBm}$ peak power (e.g. in the vicinities of ground station antennas). This leads to a total input power dynamic range of $\Delta P_{total} = 94\,\text{dB}$.

2.4.4 Gain Range Requirements for ADC Interfacing

As defined at the very beginning of this Chapter, the whole receiver can be divided into the RF frontend and baseband unit. In coordination with *Frequentis* corporation the handover interface has been defined to use an IF of 70 MHz (see Section 1.3.2).
The dynamic range of the whole receiver has been derived in Section 2.4.3 to be at least 94 dB. The ADC can cover a part of this range which depends on type in use. Thus, a closer look on the specific model used is necessary.
The baseband unit prototype utilizes an *Texas Instruments* evaluation board for the *ADS5485* 16 bit ADC featuring up to 200 million samples per second (MSPS). The noise floor of the ADC is specified to be 75 dBFS at 70 MHz[7]. The following factors have to be taken into account to determine the usable range:

- The LDACS-1 signal is supposed to have a Peak-to-Average-Power-Ratio (PAPR) of 11 dB
- An SNR of at least 4.7 dB is desired (Sec. 2.4.1), therefore, SNR_{min} is rounded up to 5 dB.
- An additional margin of 2 dB is added to account for component variation etc.

The required full-scale level of the above mentioned evaluation board is 13 dBm which yields a **required gain of** $\mathbf{G_{Frontend}} = \mathbf{21 \ldots 47\,dB}$ ($\Delta G = 26\,\text{dB}$) as illustrated in Figure 2.8.

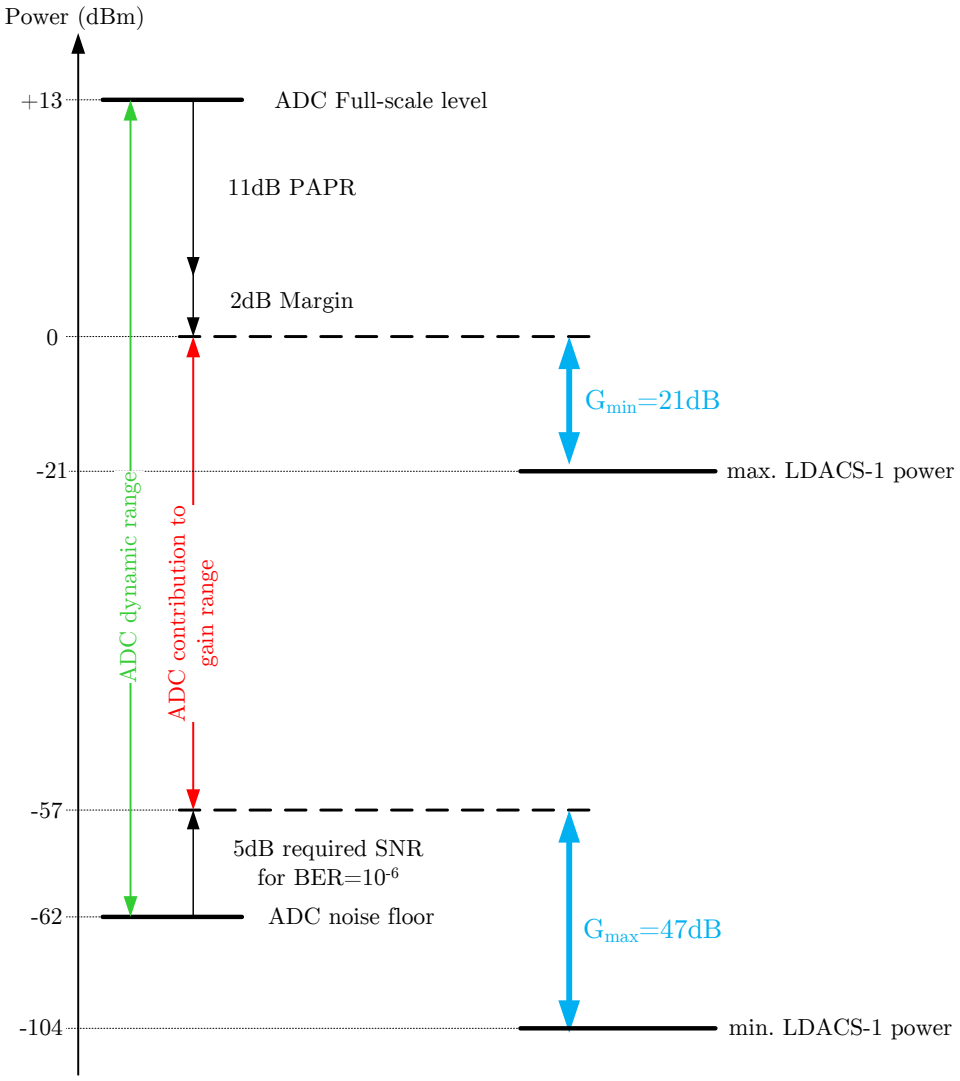

Figure 2.8: Dynamic range of ADC and the required minimal/maximal gain of the frontend.

2.4.5 Absolute Maximum Input Power

As stated in Section 2.3.1.2 the maximal power at the receiver input port will arise from DME interference. The maximum peak power the receiver has to withstand without damage are 25 dBm (23.5 dBm peak power from DME with an additional margin of 1.5 dB). Such a peak power occurrence will result in saturation of the receiver. Normal operation shall be restored after less than 2 μs (recovery time) which is not defined by the LDACS-1 standard but appointed with *Frequentis*.

2.4.6 Input 1 dB compression point P1dB

The input 1 dB compression point IP1 dB (or simply P1 dB) is desired to be at least -10 dBm. This parameter is not defined by the LDACS-1 standard but appointed with *Frequentis*.

2.5 Summary

An overview of the LDACS-1 system regarding structure and deployment options was given in Section 2.1. The receiver requirements were derived in Section 2.4 using the signal path scenarios for signals and interferers presented in Section 2.2 and 2.3. Table 2.4 shows the summarized requirements the prototype has to fulfill.

Parameter	**Value**	**Unit**
Frequency range	$960 \ldots 1164$	MHz
Channel bandwidth	0.5	MHz
Input signal power	$-104 \ldots -10$	dBm
Noise figure	≤ 5	dB
Gain	$21 \ldots 47$	dB
Abs. max. input power	25	dBm
P1dB	-10	dBm
Recovery time (after interference pulse)	≤ 2	μs

Table 2.4: Summarized requirements for the RF frontend.

Chapter 3

Receiver Design

In this chapter the general structure, as well as the advantages and disadvantages of different component arrangements, of the implemented receiver shall be discussed. Thereafter, the final component selection and a theoretical performance analysis is presented.
The receiver can be defined as the unit converting the received analog signal to the original transmitted digital bit stream. It can be divided into two main sections: The **RF frontend** delivering complex baseband signals and the **baseband unit** which is responsible for down-conversion to the baseband, demodulation, and interpreting them.
The focus of this thesis is on the frontend only, which will be referred as 'receiver' within the context of this thesis.

3.1 Receiver Structure Selection

This section first points out the difference between the two major receiver architectures—namely the Heterodyne and the Homodyne receiver—and then continues with a suitable arrangement and selection of particular components.

3.1.1 Homodyne vs. Heterodyne Receiver

The major task of the receiver is the conversion of the modulated RF signals received at the antenna port into signals that are suitable for baseband processing. For doing so, the signal has to be frequency shifted before being demodulated. This can be achieved by a direct frequency conversion to the baseband using a local oscillator (LO) at the same frequency as the signal—this concept, therefore, is often termed as the homodyne receiver. On the other hand one or more steps

can be added in which the signal is shifted to further intermediate frequencies. Both concepts bring some advantages and disadvantages which are investigated here to get a basis for a decision on which to use for the thesis.

3.1.1.1 Homodyne Structure

As mentioned before, the homodyne approach performs the desired frequency shift in a single step. It's therefore often termed as direct-conversion or zero-IF receiver. The basic structure of such a receiver can be seen in Figure 3.1.

In the first block, the frontend, the signal is bandpass (BP) filtered by a filter to protect the further stages from out-of-band interferers. This filter is followed by a low noise amplifier. Sometimes the order of both components is reversed which gives a lower NF (see Section 3.1.2) but has the drawback that the LNA in front of the chain is 'unprotected'.
The second block, the backend, performs a direct down-conversion (using the center frequency as the LO frequency) and a lowpass filtering for a suppression of the unwanted spectral parts that have not been filtered by the bandpass filter in the frontend. In Figure 3.1 the down-conversion is shown with two mixers. One is directly fed by the LO, the other with a 90 ° phase shifted version of the LO. This yields an in-phase (I) and a quadrature (Q) output so that amplitude and phase information of the signal are retained. This is called a quadrature down-conversion.

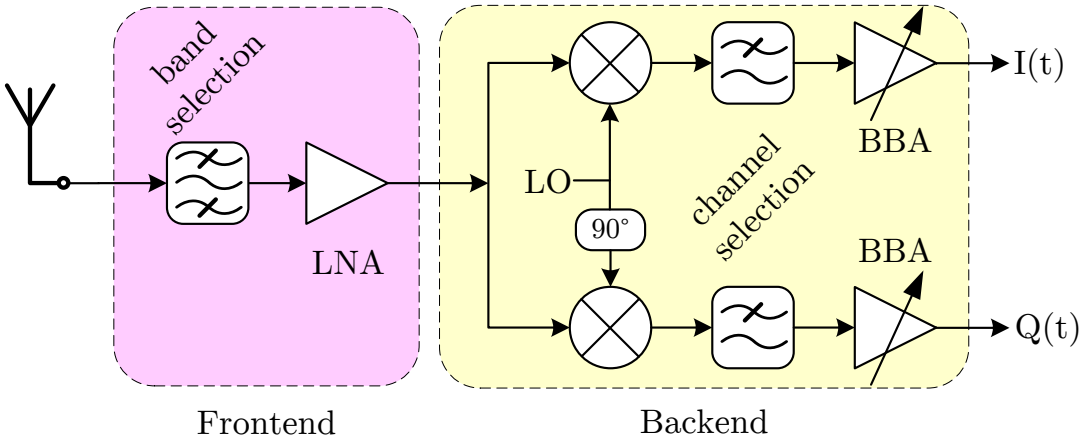

Figure 3.1: Homodyne receiver structure

Compared to other receiver structures the homodyne approach is very simple

and is, therefore, often used for applications where part count, board space, and cost are of major importance (e.g. mobile phones). Nevertheless, this structure has some disadvantages like DC offset at the mixer output and a poor immunity against interferers because of the following reasons:

- The DC offset is caused by self-mixing which has different sources:
  - Limited LO to RF isolation of the mixer, which leads to an LO leakage at the RF port
  - Limited RF to LO isolation (especially important when there are strong interferers)

  As of this limited isolations the leakages are converted down to DC. Thus a small DC offset at the mixer output experiences a large amplification by the baseband amplifiers (BBA).
- The channel selection is achieved by the lowpass filters located nearly at the end of the backend, so everything that 'fits' in the very first band selection filter will be amplified by the LNA. This is a major problem when dealing with strong interferers that are located in-band or in its vicinity.

The LDACS-1 receiver will have to operate in a rather harsh interference environment (see Section 2.3) so the look on another receiver structure is advisable.

3.1.1.2 Heterodyne Structure

The heterodyne receiver structure adds extra stages in the frequency shift process: The signal is shifted down to baseband via one or more intermediate frequencies (IFs). The general structure with one IF is shown in Figure 3.2. It can be seen that the backend looks similar to the one in the homodyne structure while the frontend is extended by an additional mixer. Adding these IF step(s) brings major advantages:

- The requirements for the quadrature downconverter and the BBAs are relaxed as they only have to deal with the (much) lower IF than the RF frequency.
- The required overall gain can be distributed over more stages. In most cases the largest part of gain—which often includes an automatic gain control (AGC) loop—is done in the IF chain. This is advantageous since the BBA can be of lower (and fixed) gain which makes the compensation of DC offsets much easier.

- The channel (pre-)selection can be done at IF where SAW filters with very steeply falling band edges (i.e. high attenuation for neighboring channels) are available. This increases the selectivity and protects succeeding stages from saturation by strong closeby interferers.

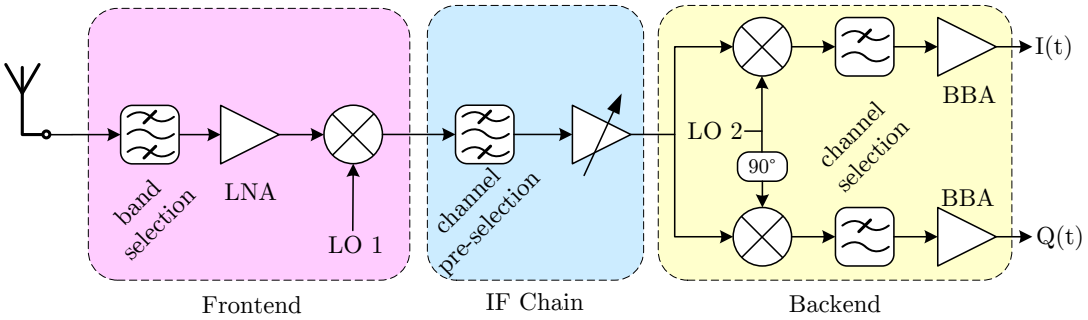

Figure 3.2: Heterodyne receiver structure

Since there are always two sides on the same coin, this structure creates a disadvantage, too, namely the so called 'image frequencies'. They originate from the mixing process (Figure 3.3) which is used for the frequency down-shift and can be described by the mathematical operation of multiplication of signals (Equation 3.1).

$$u_{\mathrm{RF}}(t) = A_{\mathrm{RF}} \cdot \cos(\omega_{\mathrm{RF}} t) \tag{3.1a}$$

$$u_{\mathrm{LO}}(t) = A_{\mathrm{LO}} \cdot \cos(\omega_{\mathrm{LO}} t) \tag{3.1b}$$

$$\begin{aligned} u_{\mathrm{IF}}(t) &= [A_{\mathrm{RF}} \cos(\omega_{\mathrm{RF}} t)] \cdot [A_{\mathrm{LO}} \cos(\omega_{\mathrm{LO}} t)] \\ &= \frac{A_{\mathrm{RF}} \cdot A_{\mathrm{LO}}}{2} [\cos(\omega_{\mathrm{RF}} + \omega_{\mathrm{LO}})\, t + \cos(\omega_{\mathrm{RF}} - \omega_{\mathrm{LO}})\, t] \end{aligned} \tag{3.1c}$$

This results in a signal (Equation 3.1c) containing the sum as well as the difference frequency of these both. This is the point where the problem arises as one signal is the LO and the second the RF input signal. Thus, frequency components which are spectrally located at $\omega_{LO} \pm \omega_{IF}$, are shifted down to the same IF frequency (Equation 3.1c) and cannot be differentiated anymore.
Figure 3.4 illustrates this fact: One of these components is the wanted signal, the other one is just noise in the best case, doubling the noise power in the band at IF. In the worst case this could also be an interferer with possibly much more power than our wanted signal making demodulation hard or even impossible.

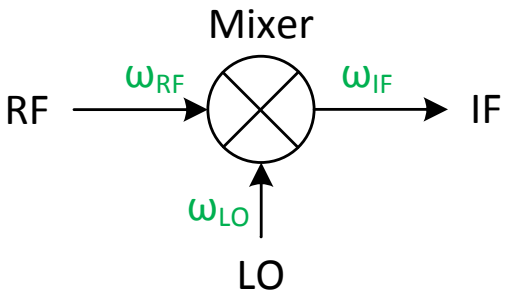

Figure 3.3: Generation of sum and difference frequency by an (ideal) mixer

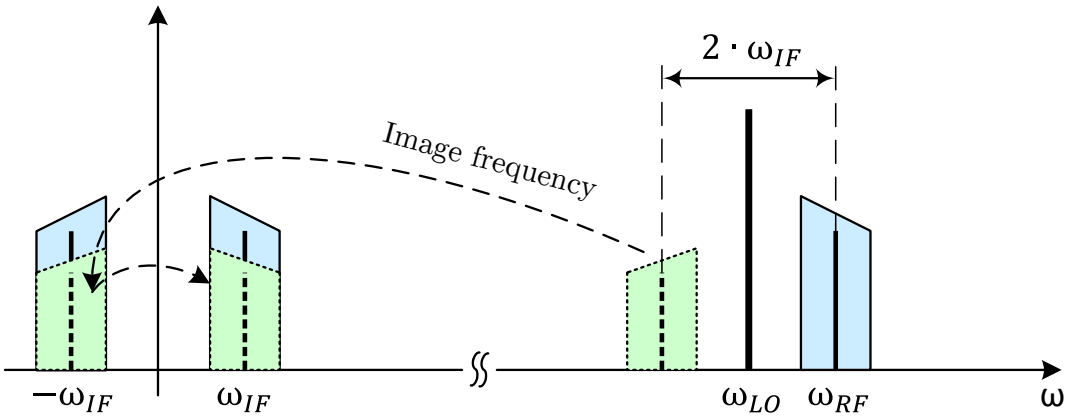

Figure 3.4: Image frequency problem

$$\omega_{\mathrm{IF}} = |\omega_{\mathrm{RF}} - \omega_{\mathrm{LO}}| \tag{3.2}$$

The problem of image frequencies is getting worse with an increasing number of IF stages, so the choice of suitable IFs is one major design challenge in heterodyne receiver structures.

Since performance has priority in the LDACS-1 receiver prototype development, the additional implementation complexity can be accepted in order to benefit from the advantages and flexibility of this architecture (e.g. higher selectivity).

Consequently, the receiver will be designed with a heterodyne structure.

3.1.2 Noise Figure Considerations

In this section the performance of the receiver chain regarding noise shall be discussed shortly. The NF plays an important role when characterizing receivers and is defined as

$$F = \frac{S_i/N_i}{S_o/N_o} \tag{3.3}$$

which is the ratio of the input and output SNR (signal-to-noise ratio) of a device and gives a measurement of how much 'extra noise' is added by a specific element. For example: the NF of a passive element (e.g. an attenuator) equals its insertion loss (IL) because the desired signal is damped by a specific amount while the noise power spectral density stays constant.
Knowing the NF and gain of each single element of the system (like amplifiers, attenuators, mixers), the overall NF of the whole chain can be calculated using the Friis' equation :

$$F_{total} = F_1 + \frac{F_2 - 1}{G_1} + \frac{F_3 - 1}{G_1 \cdot G_2} + ... + \frac{F_n - 1}{G_1 \cdot G_2 \cdot ... \cdot G_{n-1}} \tag{3.4}$$

where F_i and G_i is the NF and Gain of the i^{th} stage of the chain, respectively.

A look on this equation shows that the NF and gain of the first element(s) are dominating the properties of the whole chain. So the choice of the very first input elements is of special importance in the design process.
Therefore, a closer look on the first four stages as shown in Figure 3.2 is presented in the following:

1. Stage 1:
   The in-band IL of the **bandpass-filter or a diplexer** directly affects the NF (first term in Equation 3.4) and so must be kept low.

2. Stage 2:
   A **low noise amplifier (LNA)**, usually the second element in the chain, is used for keeping overall NF low. Modern LNA's show noise figures of around $F_{\mathrm{LNA}} \approx 0.5\,\mathrm{dB}$ or less while providing gains around $G_{\mathrm{LNA}} \approx 20\,\mathrm{dB}$.

3. Stage 3:
   The choice of the **mixer** for frequency down-conversion is (in most cases) combined with a trade-off between conversion gain/loss and linearity:

   - Active mixers provide significant conversion gain $G_{\mathrm{Mixer_{active}}} \approx 10\,\mathrm{dB}$ (typ.) while having decreased linearity compared to passive ones
   - Passive mixers come with good linearity but show high conversion loss (typ. $G_{\mathrm{Mixer_{passive}}} \approx -6 \ldots -12\,\mathrm{dB}$) and require high LO driving levels

4. Stage 4:
   The **channel selection filter** is often realized as a surface acoustic wave (SAW) filter offering high selectivity at the cost of high insertion loss compared to conventional LC filters ($G_{\mathrm{SAW}} \approx -8 \ldots -25\,\mathrm{dB}$).

As stated in Section 2.4 the LDACS-1 RX prototype requires the NF to be $F_{\mathrm{RX_{total}}} \leq 5\,\mathrm{dB}$. Stage 3 and 4 could possibly introduce an IL that drives the overall noise figure above this limit (assuming a passive mixer and a SAW filter) which has to be investigated later (see Sections 3.2.3 and 3.2.4).

3.1.3 Conclusion

Advantages and disadvantages of homodyne and heterodyne receiver structure were presented. The latter one was decided to be the basis for prototyping this LDACS-1 receiver because the heterodyne receiver generally offers higher performance, while the higher implementation complexity (i.e. part count, cost, ...) is of minor importance in this thesis. In the following section the detailed arrangement and requirements of the stages for reaching the specified performance are investigated. As the interface to the baseband unit is at IF, the receiver chain will look similar as shown in Figure 3.5.

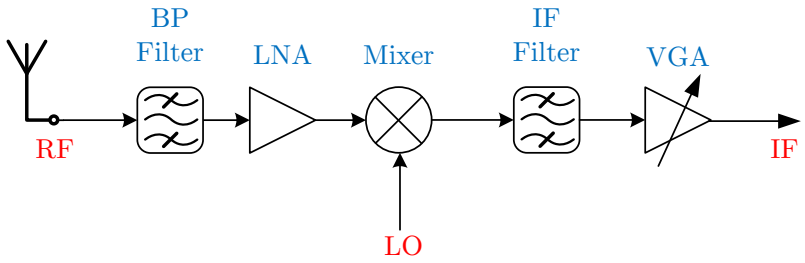

Figure 3.5: Heterodyne receiver structure, interface to baseband unit (including ADC and digital down-conversion to baseband) is at IF.

3.2 Component Selection

As the receiver structure is now fixed to a heterodyne one, the particular components for the prototype have to be chosen. When selecting these, a comparison of specific parameters of appropriate types of different vendors is performed. The most important parameters for the LDACS-1 RX are NF, P1dB, and the rather large maximum input power to 'survive' (Section 2.4.5). In the following sections the step-by-step selection process of the components is described, beginning from the RF input towards the IF output as depicted in Figure 3.5.

3.2.1 Band Selection Filter

The first element in a receiver chain usually is a bandpass-filter or a diplexer that selects the desired band (containing several channels) while attenuating out-of-band interferers and noise. In practical implementations this is sometimes challenging because the requirement for a sharp band selection (i.e. steeply falling band edges) requires filters of higher order usually introducing more loss. There are many different techniques to realize these filters (e.g. lumped elements, cavity structures, stripline) each showing different IL and transmission characteristic. The choice of the used technique mainly depends on the performance requirements, frequency range, and space constraints.

For the LDACS-1 prototype, a separate bandpass filter for each of the four possible deployment bands is used and will be provided by an external supplier (*K&L Microwave, Inc.*). Since the specifications of the LDACS-1 RX prototype do not include the band selection filter (i.e. all specifications are referenced after the BP filter) this does not affect the further component selection process. The band selection filter will, therefore, be neglected in the following.

3.2.2 Low Noise Amplifier

For the LDACS-1 frequency range there are many LNAs commercially available. Most types are, however, very limited regarding their maximal input power. The selected *SPF-5189Z* from *RFMD* [8] fulfills the mentioned maximum of +25 dBm, offers a low NF of 0.79 dB [1] and a high[2] input P1dB of 4.6 dBm compared to top of the line LNAs from other vendors.
The specified gain varies from 16.8 . . . 18.2 dB in the LDACS-1 frequency range (Figure 3.6).

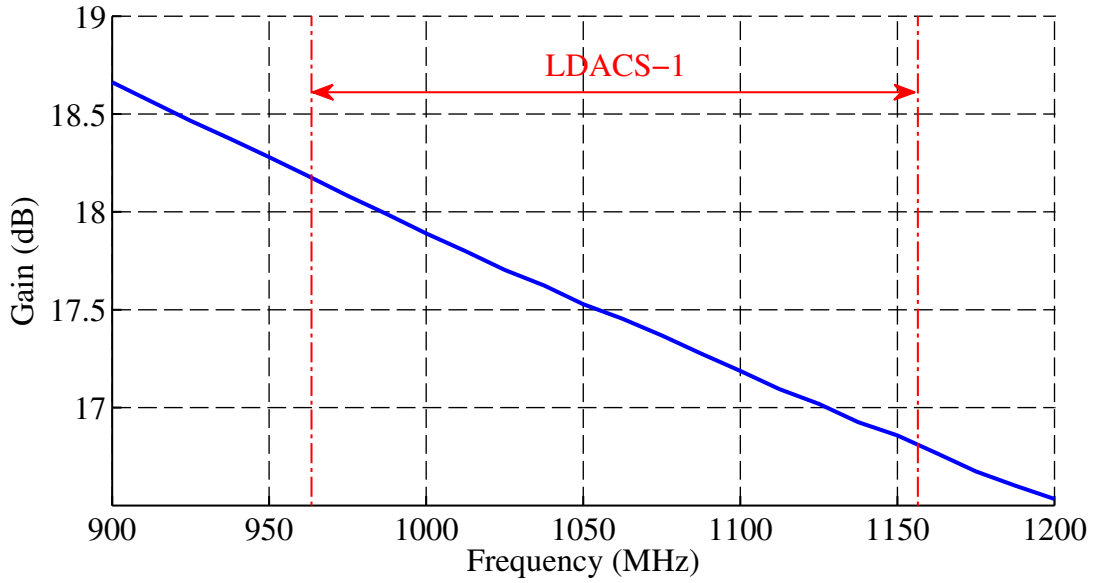

Figure 3.6: LNA gain over frequency as specified from vendor.

3.2.3 Mixer

There are two categories of mixers, active and passive ones. While active mixers often show a conversion gain $G_{\text{Mixer}} > 0\,\text{dB}$ (from RF to IF) they tend to have lower input linearity than passive ones. For this reason, a passive mixer was selected although it shows a conversion gain $G_{\text{Mixer}} < 0\,\text{dB}$ (i.e. a conversion loss). The chosen *HMC686* from *Hittite Microwave Corporation* [9] shows an input P1dB > 20 dBm which is well above the expected maximal input signal

[1] Specified in the datasheet at $f = 1.0\,\text{GHz}$.
[2] The maximal peak power of an LDACS-1 signal at the input of the receiver is specified to be −10 dBm. The 1 dB compression point of the selected LNA lies ≈ 14 dB above this level and is, therefore, considered to be sufficient.

power of 8.2 dBm[3]. When taking a look at the NF up to this point in the chain (i.e. the cascaded noise figure) in Equation 3.5 it shows that it is also well below the specified maximum.
The influence of the conversion loss of $G_{Mixer} = -7.5\,\text{dB}$[4] (typ.) onto the overall NF can be calculated by the *Friis'* equation.

$$F_{\text{LNA+Mixer}} = F_{\text{LNA}} + \frac{F_{\text{Mixer}} - 1}{G_{\text{LNA}}} \approx 1.5\,\text{dB} \tag{3.5}$$

3.2.4 IF Filter

So far the only frequency selective component in the chain is the first bandpass filter in front of the LNA that selects the desired band (see Section 3.2.1). After the down-conversion process the wanted channel has to be selected (which is the main task of this stage) and the rest should be filtered. The output signal of the mixer not only contains other in-band channels, interferers, and noise but also new unwanted spectral components that are generated by the mixer due to nonlinearity, namely the spurious products. These intermodulation products arise at predetermined frequencies

$$f_{OUT} = n \cdot f_{LO} + m \cdot f_{RF} \quad \forall n, m \in \mathbb{Z} \tag{3.6}$$

that have to be filtered, too (in order not to saturate or influence any further stages), which is also job of the IF filter.
Just as for the band selection filter in Section 3.2.1, there are many realization techniques possible here. However, the most common type used are SAW filters since they show a highly selective frequency response (i.e. bandpass characteristic with steeply falling band edges) that make them ideal for channel selection. A drawback of SAW technology is the relatively high IL and a rather low maximal power handling compared to other filter type (e.g. LC, stripline).
The selected filter type is the *'854651'* from *TriQuint Semiconductor, Inc.* [10] (former *SAWTEK*) showing an in-band IL of $G_{\text{SAW}} = -7.6 \ldots -10.87\,\text{dB}$ which has the effect that the LDACS-1 OFDM subcarriers located near the edges of the channel experience up to 3.27 dB more attenuation than other ones as depicted in Figure 3.7. Furthermore, the maximal input power is not specified for the selected filter and, hence, has to be verified (Section 3.3.4.1). Typical values for

[3]Since the LNA does not provide more than 18.2 dB gain in the LDACS-1 frequency range, the maximal signal peak power at the mixer input will be $\leq 8\,\text{dBm}$.

[4]The NF of the mixer is specified in the datasheet as single sideband (SSB) NF to be typically 7.5 dB. Since there is no filter foreseen before the mixer to suppress the second sideband, the NF doubles and is, therefore, calculated with $F_{\text{Mixer}} \approx 10.5\,\text{dB}$. For this assumption, the spectral contents in the second sideband are assumed to be white noise only. For the LNA, the lowest gain in the LDACS-1 frequency range of 16.8 dB was used for calculations.

comparable types are about 10 dBm.

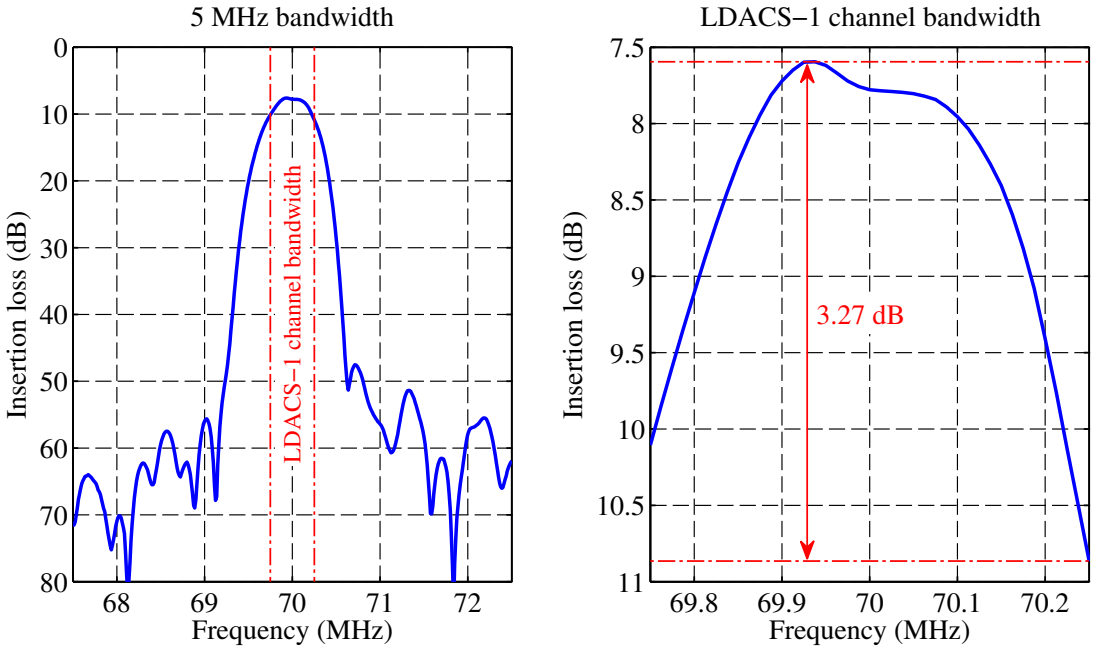

Figure 3.7: SAW filter insertion loss over frequency as specified from vendor.

As the type of the channel selection filter is selected now, a look on the compliance with the specifications is necessary. For calculation of the cascaded NF the highest attenuation of the SAW filter at the band edges $G_{\mathrm{SAW}_{\max}} = -10.87\,\mathrm{dB}$ is used as a worst case estimate (i.e. the NF averaged over the channel will be less than this). This value has to be used as NF of the filter $F_{\mathrm{SAW}} = -G_{\mathrm{SAW}_{\max}}$ when inserting into the *Friis'* formula.

$$F_{\mathrm{LNA+Mixer+SAW}} = F_{\mathrm{LNA}} + \frac{F_{\mathrm{Mixer}} - 1}{G_{\mathrm{LNA}}} + \frac{F_{\mathrm{SAW}} - 1}{G_{\mathrm{LNA}} \cdot G_{\mathrm{Mixer}}} \approx 4.37\,\mathrm{dB} \tag{3.7}$$

As seen in Equation 3.7, the overall NF up to this stage rises to $\approx 4.37\,\mathrm{dB}$ which is near the specified maximum. As this leaves almost no headroom for any additional stages by which the NF only can be increased, a modification of the structure shown in Figure 3.5 is necessary. For a decreased NF an amplifier introducing gain is needed in front of the SAW filter.

For this reason, the following section presents a modified structure which introduces a variable gain amplifier after the mixer.

3.2.5 Variable Gain Amplifier

In the previous Section the need for an amplifier in front of the SAW filter—in order to decrease the noise figure—was derived. Using a variable gain amplifier for this task simultaneously covers the required gain dynamic range of the receiver ($\Delta G = 26\,\text{dB}$ as derived in Section 2.4.4). The gain shall be adjustable with an external control voltage as coordinated in the course of the project with *Frequentis* in order to implement an automatic gain control (AGC) operated by the baseband unit.

The selected VGA type is the *'AD8367'* from *'Analog Devices, Inc.'* [11]. It basically consists of a fixed gain amplifier providing 42.5 dB gain and a preceding variable attenuator which provides a dynamic range of about 45 dB. The minimal NF of 7.5 dB is achieved at maximal gain and increases in an one-to-one relation to decreasing gain (i.e. the NF increases 1 dB for every 1 dB reduction in gain). Equation 3.8a shows the decreased NF of $\approx 2.92\,\text{dB}$ when swapping the positions of the SAW filter and the VGA as depicted in Figure 3.8a. However, this structure has one drawback: All intermodulation products of the mixer directly enter the input of the VGA and, thus, get amplified or might lead to saturation or other unwanted side effects.
An approach that might eliminate this drawback, while keeping the decreased NF, is the insertion of a filter with lower IL that is not as frequency selective as a SAW filter but suppresses these unwanted products (Figure 3.8b).
The datasheet of the mixer provides a table of these spurious products' power up to 8^{th} order ($n, m \in \{1 \dots 4\}$ in Equation 3.6). So they are assumed to arise only in the frequency range of 240.75 MHz[5] and 4974 MHz[6]. Products of higher order are supposed to be of much less power and are neglected, therefore.
The concatenation of three filters from *'Mini-Circuits'* (Figure 3.9) provides high suppression in this range while keeping the in-band IL low. Each of the filters provides the desired attenuation in a different part of the frequency range of the spurious products (Figure 3.10). The bandpass filter *'SXBP-70+'* [12] covers the lower frequencies while the lowpass filters *'LFCN-1200'* [13] and *'LFCN-3000'* [14] cover the upper ones. This combination provides a suppression better than 37 dB[7] in the range of about 170 MHz ... 7 GHz whereas the in-band IL—and so the combined noise figure of these filters—is less than $G_{SF} \geq -1.1\,\text{dB}$.

[5] $f_{RF} = 963.5\,\text{MHz}, f_{LO} = 893.5\,\text{MHz}, n = 4, m = -1$
[6] $f_{RF} = 1156.5\,\text{MHz}, f_{LO} = 1226.5\,\text{MHz}, n = 1, m = -4$
[7] The BP filter *SXBP-70+* is specified till 2.5 GHz, thereafter it is assumed that it provides no IL.

$$\begin{aligned} F_{\text{LNA+Mixer+VGA+SAW}} &= F_{\text{LNA}} + \frac{F_{\text{Mixer}} - 1}{G_{\text{LNA}}} + \frac{F_{\text{VGA}} - 1}{G_{\text{LNA}} \cdot G_{\text{Mixer}}} \\ &\quad + \frac{F_{\text{SAW}} - 1}{G_{\text{LNA}} \cdot G_{\text{Mixer}} \cdot G_{\text{VGA}}} \\ &= 1.1995 + 0.2135 + 0.5432 + 74.117 \cdot 10^{-6} \\ &= 1.95663 \approx \mathbf{2.92\,dB} \end{aligned} \tag{3.8a}$$

$$\begin{aligned} F_{\text{LNA+Mixer+SF+VGA+SAW}} &= F_{\text{LNA}} + \frac{F_{\text{Mixer}} - 1}{G_{\text{LNA}}} + \frac{F_{\text{SF}} - 1}{G_{\text{LNA}} \cdot G_{\text{Mixer}}} \\ &\quad + \frac{F_{\text{VGA}} - 1}{G_{\text{LNA}} \cdot G_{\text{Mixer}} \cdot G_{\text{SF}}} \\ &\quad + \frac{F_{\text{SAW}} - 1}{G_{\text{LNA}} \cdot G_{\text{Mixer}} \cdot G_{\text{SF}} \cdot G_{\text{VGA}}} \\ &= 1.1995 + 0.2135 + 0.0339 \\ &\quad + 0.6998 + 95.479 \cdot 10^{-6} \\ &= 2.1467 \approx \mathbf{3.32\,dB} \end{aligned} \tag{3.8b}$$

The resulting cascaded NF $F_{\text{LNA+Mixer+SF+VGA+SAW}} \approx 3.31\,\text{dB}$ (Equation 3.8b) has only slightly increased by 0.39 dB. The remaining 1.69 dB margin (to the maximum of 5 dB) is supposed to be sufficient for the further stages as well as implementation losses (connectors, PCB interconnects, etc.).

Thus, selection of components for the receiver chain as depicted in Figure 3.8b is finished. At this stage, the chain now provides a defined gain, down-conversion, channel selection, and a VGA that covers the required gain dynamic range of $\Delta G = 26\,\text{dB}$. What still remains is to extend this structure by fixed gain amplifiers in order to provide the required absolute gain (Figure 2.8) which is topic of the next section.

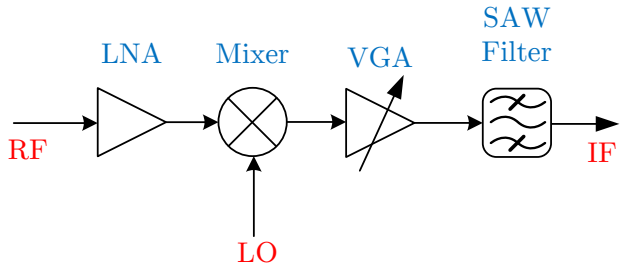

(a) Swapped arrangement of SAW filter and VGA.

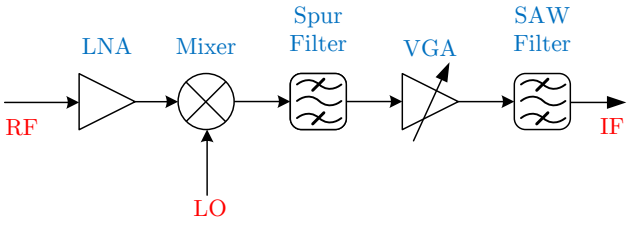

(b) Additional 'spur filter' after the mixer for mixer spurious product suppression.

Figure 3.8: Modified heterodyne receiver structure in order to fulfill the NF specifications.

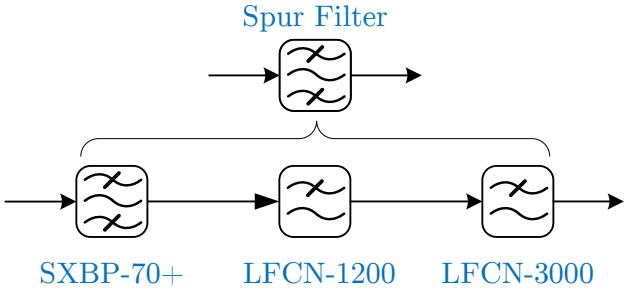

Figure 3.9: Spur filter for suppression of unwanted intermodulation products from the mixer.

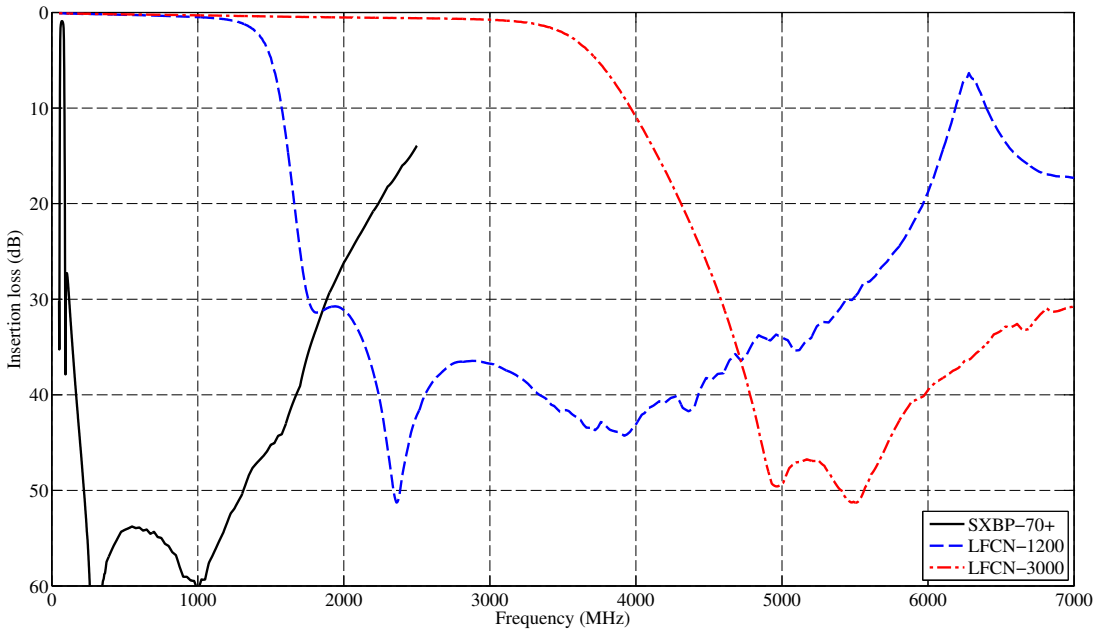

(a) Frequency response of the three selected IF filters.

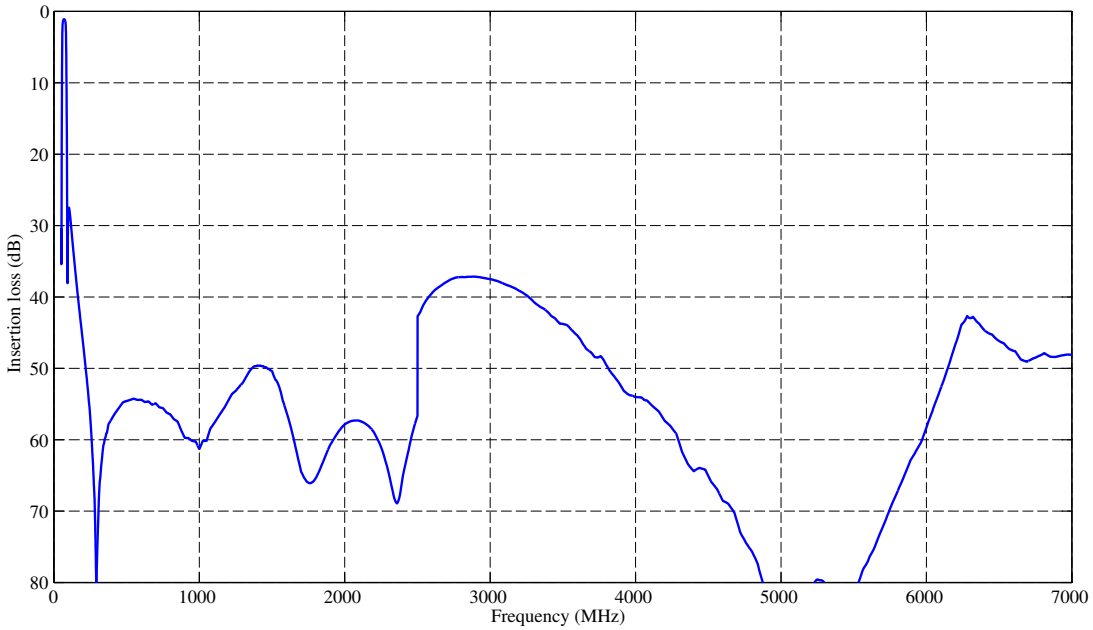

(b) Frequency response of the concatenation of the three IF filters.

Figure 3.10: Frequency response of the three IF filters for mixer spurious product suppression. The bandpass filter *SXBP-70+* is specified up to 2.5 GHz from the vendor and is, therefore, considered to add no further spurious product suppression beyond this frequency. The concatenation of the filters shows an attenuation > 37 dB in the frequency range of about 170 MHz . . . 7 GHz.

3.2.6 IF Gain Stage

As implied in the preceding section, an adjustment of the absolute gain level is done by another extension of the chain. This will consist of a fixed gain stage followed by an SAW channel selection filter (Figure 3.11). The same type of filter as selected in Section 3.2.4 is used. This second channel filter originates from a request by *Frequentis* to increase the channel selectivity. Although the filter shows a remarkable IL it does not contribute much to the overall NF because of it's position at the very end of the chain.

$$\begin{aligned} G_{\text{Final}} = & \underbrace{G_{\text{LNA}}}_{16.8\ldots18.2\,\text{dB}} + \underbrace{G_{\text{Mixer}}}_{-7.5\,\text{dB}} + \underbrace{G_{\text{SpurFilter}}}_{-1.1\,\text{dB}} + \underbrace{G_{VGA}}_{-2.5\ldots42.5\,\text{dB}} + \underbrace{2 \cdot G_{\text{SAW}}}_{2\cdot(-7.6\ldots-10.87\,\text{dB})} + G_{\text{IF Stage}} \\ & = G_{\text{freq}} + G_{\text{adj}} + G_{\text{IF Stage}} \\ & = \underbrace{(-5.6\ldots-13.54\,\text{dB})}_{\text{frequency dependent}} + \underbrace{(-2.5\ldots42.5\,\text{dB})}_{\text{adjustable}} + G_{\text{IF Stage}} \end{aligned} \tag{3.9}$$

The gain of this (final) structure is given by Equation 3.9. The ranges arise from two parts: A frequency dependent part (mainly caused by the SAW filters and the LNA) and an adjustable part by the VGA. The required gain of the IF gain stage is now to be determined so that the desired maximum gain of $G_{max} = 47\,\text{dB}$ is fulfilled for all specified frequencies. So for the calculation the lowest value in the frequency dependent part and the highest gain of the VGA (in order to keep the NF low) have to be considered. The resulting minimal gain of $G_{\text{IF Stage}} \geq 18.04\,\text{dB}$ is then given by Equation 3.10.

$$\begin{aligned} G_{\text{IF Stage}} &\geq G_{\max} - \min\left(G_{\text{freq}}\right) - \max\left(G_{\text{adj}}\right) \\ &= 47\,\text{dB} + 13.54\,\text{dB} - 42.5\,\text{dB} = 18.04\,\text{dB} \end{aligned} \tag{3.10}$$

As depicted in Figure 3.11 this stage consists of two gain blocks separated by an attenuator (ATT) in order to have an opportunity to tune the final gain. The chosen *'ADL5536'* [15] and *'ADL5535'* [16] from *'Analog Devices, Inc.'* are common IF gain blocks and only differ in their provided fixed gain of 20 dB and 16 dB, respectively. The attenuator is a Π-type resistor network and is initially dimensioned to offer $G_{\text{ATT}} = -10\,\text{dB}$ so that the complete IF gain stage offers 26 dB gain. This is about 8 dB more than required to leave some margin for implementation losses and, therefore, might be adapted later.

3.3 Performance Analysis of the Receiver

What remains is to analyze the properties of the components selected in the previous section in their final arrangement (Figure 3.11). This is to see if they

match the LDACS-1 specifications (Table 2.4).

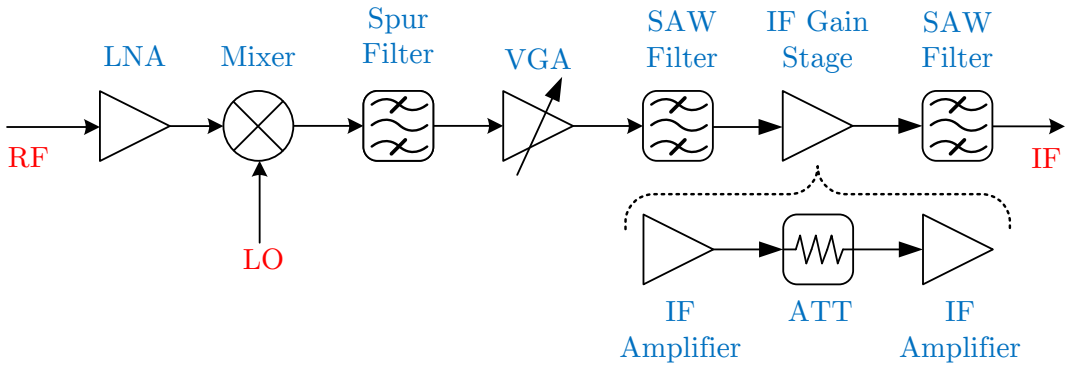

Figure 3.11: Final structure of the LDACS-1 receiver frontend. The SAW filter at the very end of the chain improves channel selectivity.

3.3.1 Noise Figure

The IF gain stage and the SAW filter introduced in Section 3.2.6 are supposed to nearly have no effect on the NF as they are after the VGA which provides a lot of gain. This is emphasized in Figure 3.12, by plotting the cascaded NF after each stage, and in Equation A.1 in Appendix A showing the tiny contribution of the terms at the very end.
The overall calculated noise figure of $\mathbf{F}_{\text{total}} = \mathbf{3.32\,dB}$ surpasses the specified maximum of 5 dB by far.

3.3.2 Gain Range

As derived in Section 2.4.4, the required overall gain range is $G_{\text{Frontend}} = 21...47\,\text{dB}$. The total gain range is presented in Equation 3.11 and obviously covers the requirements[8].

$$\mathbf{G_{RX}} = \underbrace{\mathbf{13.93\ldots58.93\,dB}}_{\text{adjustable}} \quad \underbrace{\mathbf{\pm 3.97\,dB}}_{\text{frequency dependent}} \tag{3.11}$$

3.3.3 Input 1 dB Compression Point (P1dB)

The input 1 dB compression point IP1 dB (or simply $P1\,\text{dB}$) identifies the power that is necessary to saturate an element or device (usually an amplifier) as far

[8]The gain range is derived from Equation 3.9 assuming $G_{\text{IF Stage}} = 26\,\text{dB}$.

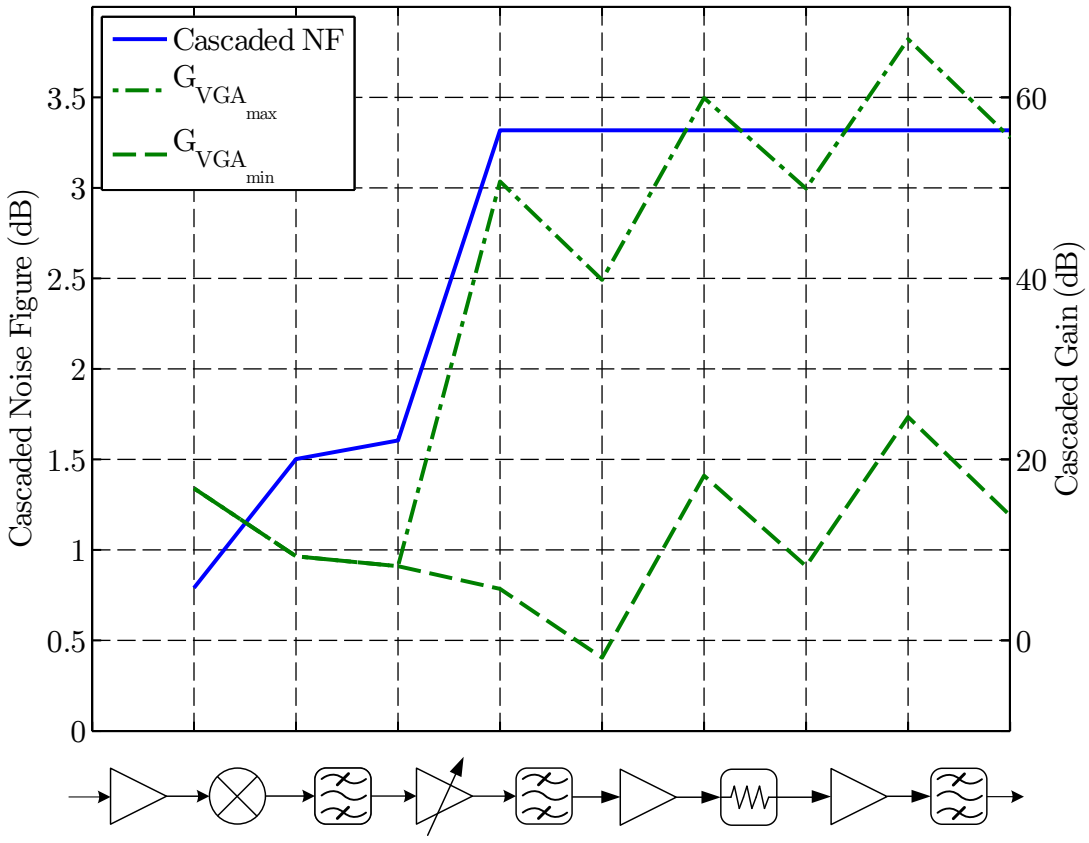

Figure 3.12: Cascaded noise figure and gain of the realized receiver.

as its gain decreases by 1 dB. For the LDACS-1 RX this point is desired to be $P1\,\mathrm{dB} \geq -10\,\mathrm{dBm}$ (Section 2.5).
For an evaluation of $P1\,\mathrm{dB}$ the input power that results in reaching the $P1\,\mathrm{dB}$ of a single component is of interest. For this reason the cascaded gain shown in Figure 3.12 for minimal VGA gain ($G_{\mathrm{VGA_{min}}}$) is calculated using the minimum IL for the SAW filters $G_{\mathrm{SAW_{min}}} = -7.6\,\mathrm{dB}$. As the $P1\,\mathrm{dB}$ is only applicable for high input power levels, the VGA is assumed to be set for minimum gain $G_{\mathrm{VGA_{min}}} = -2.5\,\mathrm{dB}$. The resulting $P1\,\mathrm{dB_{RX}}$ of the complete receiver chain is then determined by the lowest value of $P1\,\mathrm{dB} - G_C$ as calculated in Table 3.1.

Function	**Component**	$\mathbf{IP_{1\,dB}}$ (dBm)	**Casc. Gain** $\mathbf{G_C}$ (dB)	$\mathbf{P1\,dB - G_C}$ (dBm)
LNA	SPF-5189z	4.3	0	4.3
Mixer	HMC686LP4	25	18.2	6.8
VGA	AD8367	1	6	−5
IF Amp. 1	ADL5536	−0.5	−0.5	0
IF Amp. 2	ADL5535	2.4	9.6	**−7.2**

Table 3.1: Summarized values for $P1\,\mathrm{dB}$ of the selected components, the cascaded gain G_C at their inputs, and the input power $P1\,\mathrm{dB} - G_C$ to reach the compression point for the specific component. The second IF amplifier is supposed to saturate first. The $P1\,\mathrm{dB}$ of the chain is, therefore, given as about $-7.2\,\mathrm{dBm}$.

The minimum of these values occurs at the second IF amplifier and determines the overall to $\mathbf{P1\,dB_{RX} = -7.2\,dBm}$ which is about 3 dB above the specification. In this consideration the filters are disregarded since they are supposed to show no nonlinearity at this power levels and, thus, have no applicable $P1\,\mathrm{dB}$.

3.3.4 Absolute Maximum Input Power

The receiver has to withstand an input power of 25 dBm without damage (Section 2.4.5). This has to be made sure for all operational states (e.g. even when the VGA is at maximal gain). The resulting maximal input power levels for each component in the chain are depicted in Figure 3.13. Note that all amplifiers are saturated in this case and hence do not provide the gain as in normal operation[9]. The maximum power levels as depicted in the upper trace in Figure 3.13 (without

[9]Saturated output power levels of the amplifiers: $P_{\mathrm{LNA_{SAT}}} = 22\,\mathrm{dBm}$, $P_{\mathrm{VGA_{SAT}}} = 9\,\mathrm{dBm}$, $P_{\mathrm{IFAmp1_{SAT}}} = P_{\mathrm{IFAmp2_{SAT}}} = 20\,\mathrm{dBm}$

the limiter diode) do not fulfill the specifications for the SAW filter as well as for the VGA. Possible solutions are presented in the following Sections 3.3.4.1 and 3.3.4.2, respectively.

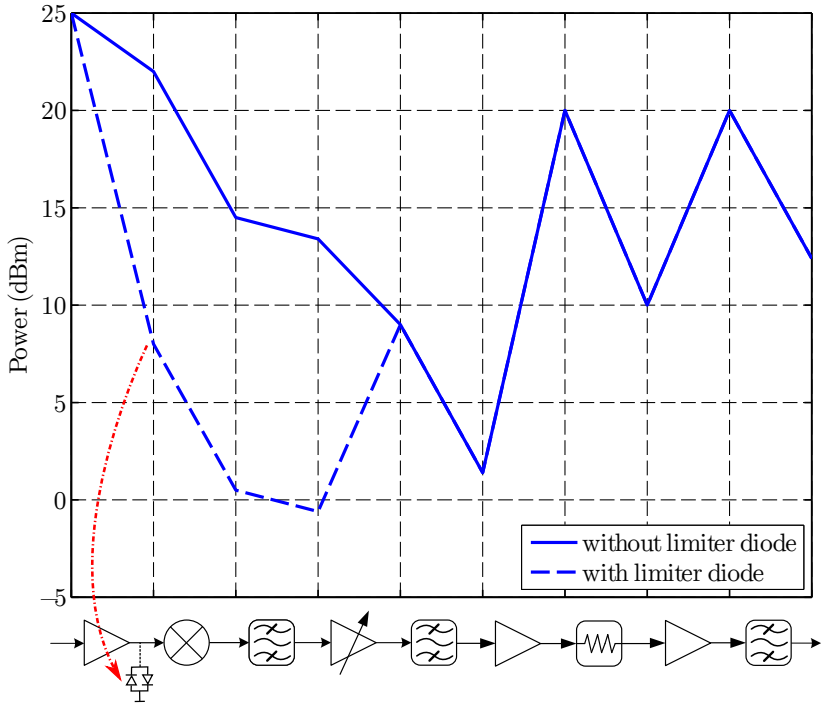

Figure 3.13: Power at each node for $P_{\text{in}} = 25\,\text{dBm}$[10]. The insertion of limiter diodes after the LNA protects the VGA from too much power.

3.3.4.1 SAW filter

The maximal input power into the selected SAW filter $P_{\text{SAW}_{\text{max}}} = P_{\text{ADL5535}_{\text{SAT}}} = 20\,\text{dBm}$ occurs due to saturation of the second fixed gain IF amplifier (Figure 3.13). The maximal input power of the filter lacks specification (Section 3.2.4) and, so, must be verified since most of comparable filter types are rated for 10 dBm only.

The internal structure of an SAW filter consists of interleaved metal electrodes used to transmit/receive waves on a piezoelectric substrate (Figure 3.14). The thin metallic fingers are supposed to get destroyed when stressed with too much RF power. As it is supposed that higher ambient temperatures could cause a destruction at even lower RF power, a measurement setup is introduced that allows simultaneous RF power and thermal stress as illustrated in Figure 3.15.

Therefore, the SAW filter is mounted in a test fixture that consists of a milled

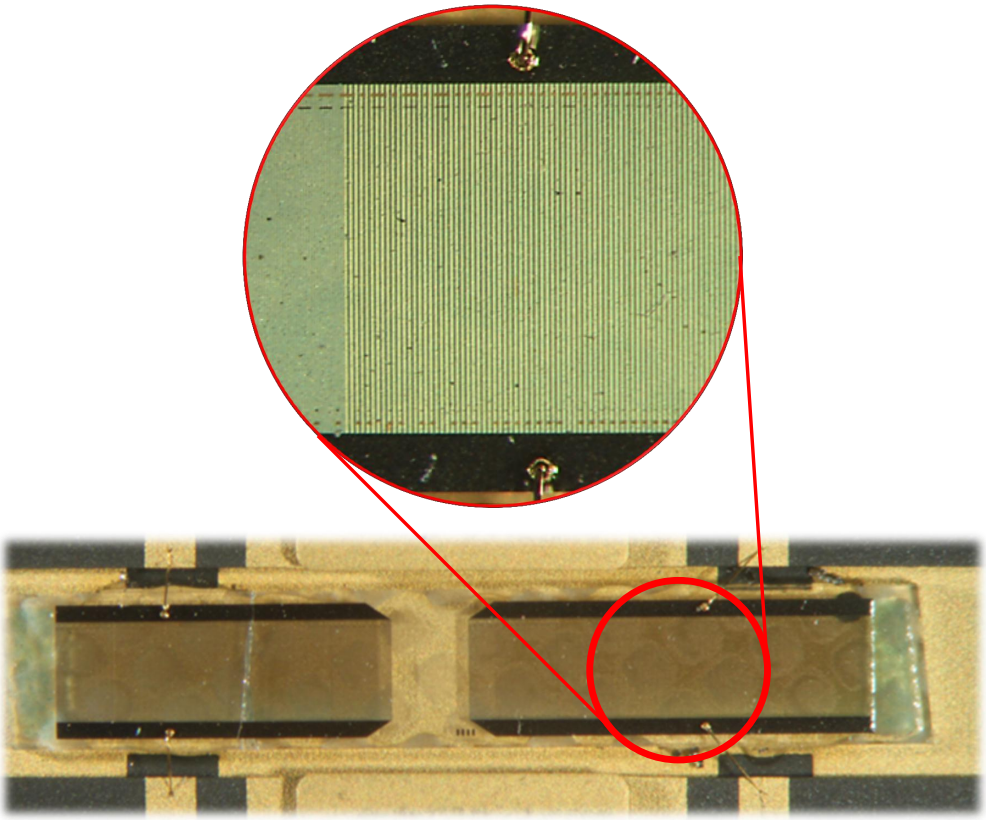

Figure 3.14: Inner structure of the filter. It consists of very thin interleaved metal electrodes on a Quartz substrate. The crack on the left side originates from opening the filter. The thin metallic 'fingers' are supposed to incinerate when impinged with too much RF power.

PCB, lumped components for impedance matching to 50 Ω, and SMA connectors as seen in Figure 3.16. It is then placed into a temperature chamber keeping a constant ambient temperature of 50 °C and stressed with 20 dBm RF power[11]. After 24 hours[12] the transfer function is compared to the one right before the stress-test to see possible influences. As there was no noticeable change it can be assumed that the SAW filter will withstand the maximal power required for the LDACS-1 receiver.

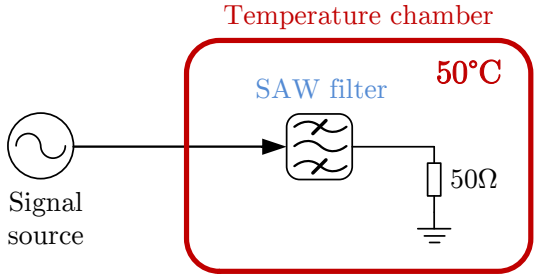

Figure 3.15: Setup for simultaneous RF power and thermal stress of the SAW filter.

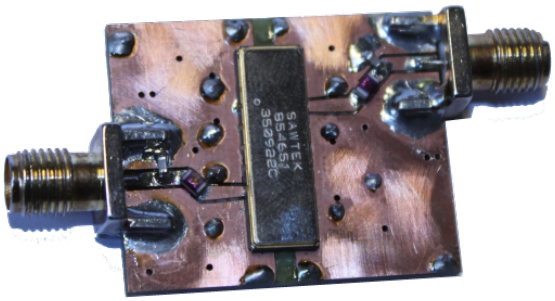

Figure 3.16: Test fixture for power handling verification.

3.3.4.2 VGA

The maximal input power into the variable gain amplifier is given by $P_{\mathrm{VGA}_{\mathrm{max}}} = P_{\mathrm{LNA}_{\mathrm{SAT}}} - G_{\mathrm{Mixer}} - G_{\mathrm{SpurFilter}} = 13.4\,\mathrm{dBm}$ (Figure 3.13). The *AD8367* is specified to withstand an input voltage of ±600 mV. A 1:2 Balun is used for input matching to 50 Ω and so ±300 mV (or about 0 dBm) are acceptable at the input.
This creates the need for an additional protection mechanism. A possible solution is the insertion of two limiter diodes *SMP1330* from *Skyworks Solutions,*

[11] $f = 70\,\mathrm{MHz}$, continuous wave signal
[12] It is supposed that a longer period will not change the result.

Inc. after the LNA. They reduce the input power into the mixer from 13.4 dBm to less than 0 dBm (Figure 3.13) and so protect the VGA from damage. The input/output power relation of these diodes is depicted in Figure 3.17.
They introduce an insertion loss of < 0.4 dB at signal powers levels. Therefore, their influence is neglected for further power level and linearity considerations.

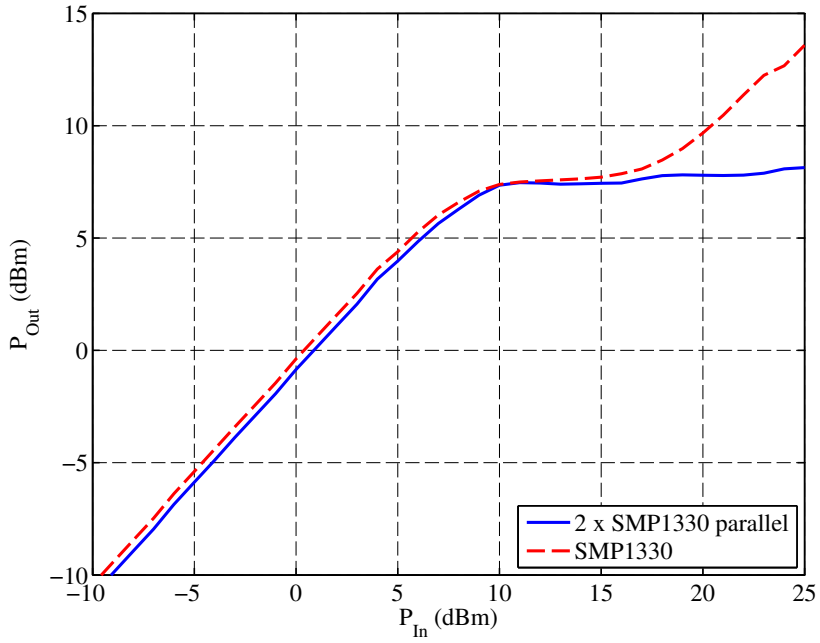

Figure 3.17: P_{out} over P_{in} for the limiter diode SMP1330. A parallel arrangement of two diodes increases attenuation at high input power levels.

3.3.5 Link Budget

To complete the performance analysis, the link budget of the receiver chain is presented. Figure 3.18 provides an overview of signal and noise power at each node in lowest and highest gain operation. For the lowest input power the SNR is given to about $\mathrm{SNR}_{\mathrm{min}} \approx 8\,\mathrm{dB}$ which outperforms the required 4.7 dB (Section 2.4.1).

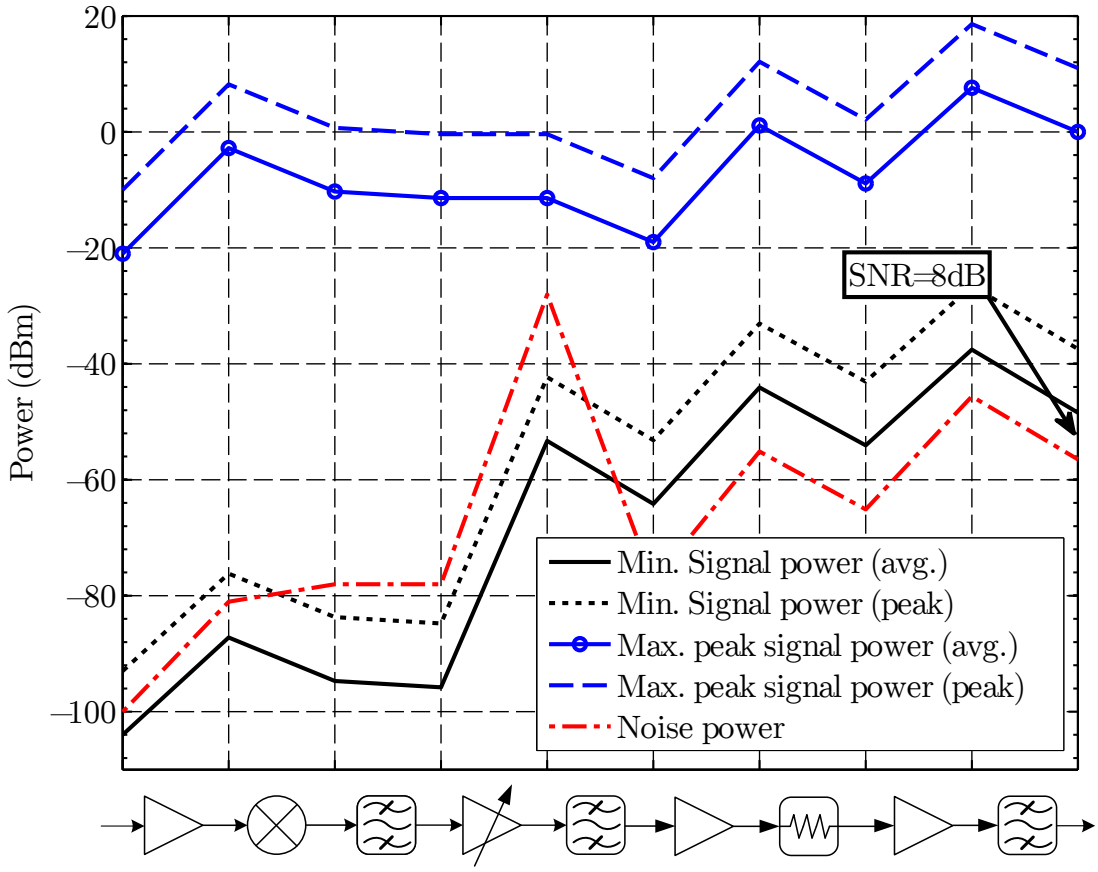

Figure 3.18: Power at each node for $P_{\mathrm{in}} = 25\,\mathrm{dBm}$ ($G_{\mathrm{VGA}} = \mathrm{max.}$). All amplifiers in the chain are saturated and, thus, don't show their normal gain.

3.4 Summary

In this chapter the general structure of the receiver and afterwards the particular components were selected. During the design process it turned out that a modified structure as seen in Figure 3.8b is beneficial for reduction of the noise figure which leads to the final component arrangement as depicted in Figure 3.11. A performance analysis of the complete receiver chain is presented showing that the prototype is supposed to meet or even exceed the LDACS-1 specifications.

Chapter 4

Receiver Chain Measurements

The practical implementation of the derived receiver structure shall now be shown. In the hardware prototyping process it has been found advantageous to build test fixtures for each component in the receiver chain. These allow easier verification and debugging (Figure 4.1). The arrangement was briefly checked for functionality and basic measurements were done using these test fixtures. A PCB containing the complete setup of the whole chain was designed and manufactured. The following presented measurements were performed using this board (Figure 4.2).

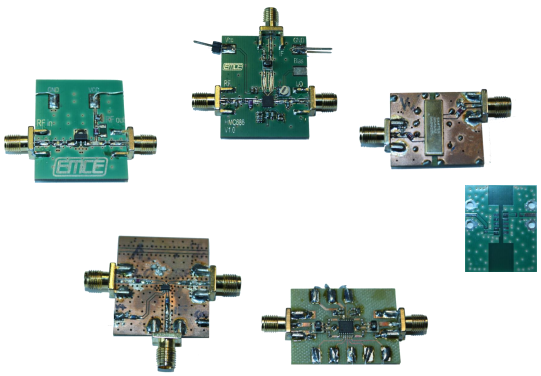

Figure 4.1: Implemented test fixtures for verification and performance measurements.

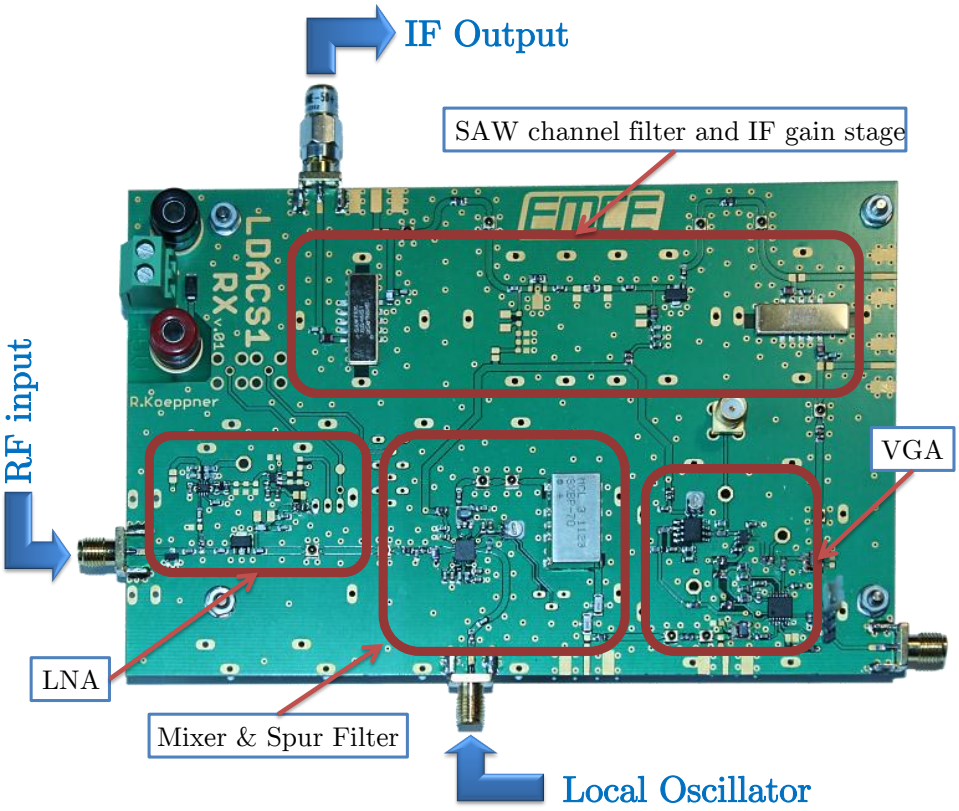

Figure 4.2: PCB of the LDACS-1 receiver frontend prototype.

4.1 Verification measurements

This section shall verify if the presented prototype fulfills the LDACS-1 requirements.

4.1.1 Gain

In Section 2.4.4 the required gain range of $G_{\text{Frontend}} = 21 \ldots 47\,\text{dB}$ was derived. A measurement setup as illustrated in Figure 4.3 was utilized for gain measurements. An LDACS-1 test signal with defined power level is generated utilizing a *Rohde&Schwarz SMBV100A* signal source[1] and fed into the receiver prototype. The gain is determined by the ratio of input to output power (both measured by a power meter).
Figure 4.4 shows the measured gain in dependence of the control voltage of the VGA[2]. It ranges from $\mathbf{6.7 \ldots 52.4\,dB}$ (967 MHz) and $\mathbf{10.2 \ldots 55.4\,dB}$ (1163 MHz) which is slightly under the calculated values from Section 3.3.2, most likely caused by implementation losses (e.g. PCB interconnects).

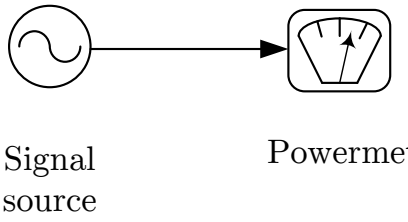

(a) Power meter directly connected to the signal source for absolute power calibration.

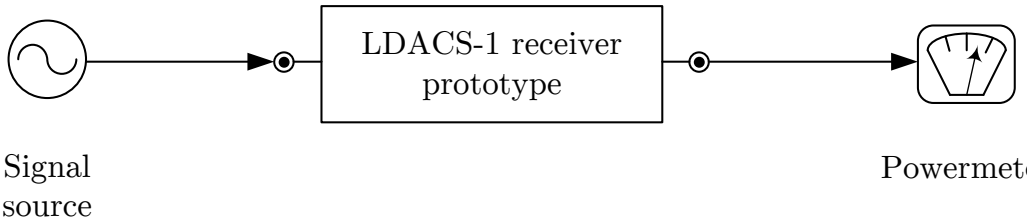

(b) Determination of the gain by inserting the receiver prototype between signal source and power meter.

Figure 4.3: Measurement setup for determining the gain.

[1]The Rohde&Schwarz SMBV100A signal source allows the generation of arbitrary waveforms. LDACS-1 exemplary I/Q data, provided by Frequentis, were used for modulation. The output power was calibrated using a power meter.
[2]Measured with a LDACS-1 signal.

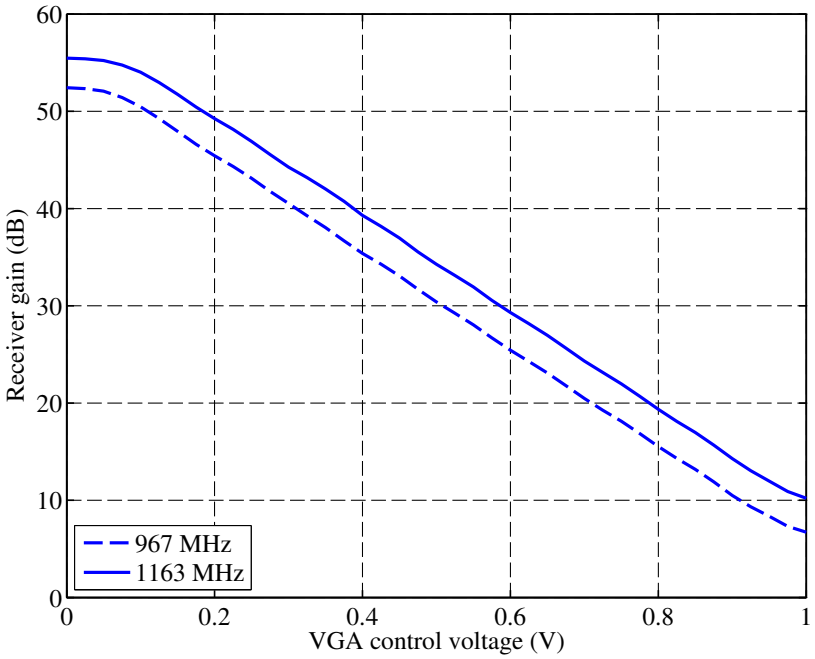

Figure 4.4: Gain over control voltage of the VGA. Lowest and highest LDACS-1 deployment band show slightly different gain mainly influenced by LNA frequency dependence.

4.1.2 P1dB

The 1 dB compression point is defined to be at least the same level of the maximal signal peak power ($\text{P1dB}_{\text{desired}} \geq -10\,\text{dBm}$). It can be determined using the same setup as before (Figure 4.3). For this type of measurement, a CW signal is used instead of an LDACS-1 signal as the latter shows a significant PAPR[3].
Figure 4.5 shows output power in dependence of the input power, measured at minimal VGA gain, and the corresponding **P1dB of about −9.5 dBm** which is slightly above the specified −10 dBm.

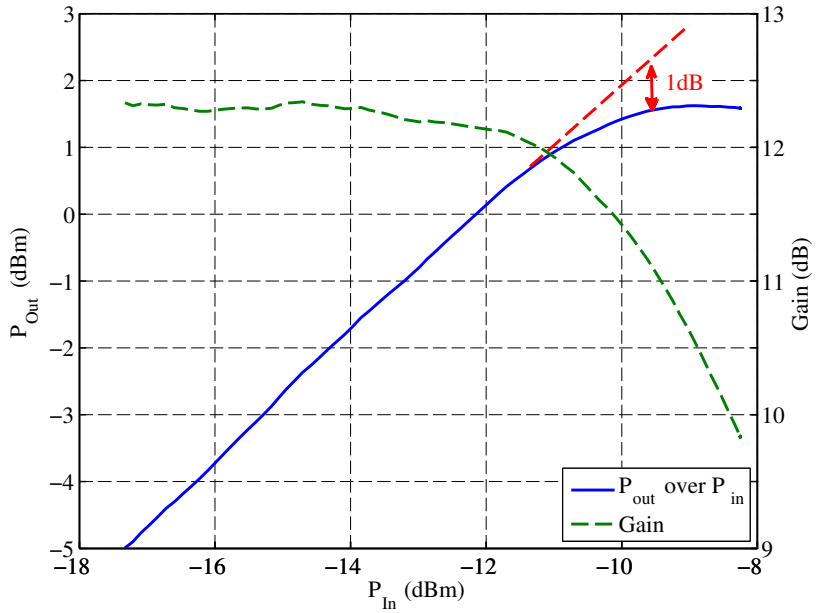

Figure 4.5: P_{out} over P_{in} measured at 1163 MHz, showing that the 1 dB compression point is slightly above the required −10 dBm. The measurement was performed at minimal VGA gain.

4.1.3 Noise Figure

4.1.3.1 The Hot/Cold Method

There are various methods for measuring the noise figure. One of them is the hot/cold method (also known as Y-factor method) which utilizes a so called *Noise Source*. The source provides a well defined noise power level when it's powered or

[3]When using an LDACS-1 signal for this type of measurement, the compression of the signal peaks do not affect the total output power much and, thus, do not lead to the desired measurement.

not. It corresponds to thermal noise at a hot T_{hot} or ambient temperature T_{cold}, respectively. The *Excess Noise Ratio* (ENR) defines the 'hotness' of a specific noise source as difference between T_{hot} and T_{cold} divided by 290 Kelvin (Equation 4.1) and is specified by the manufacturer. As a rule of thumb, this method provides accurate measurements for all devices with no more than $\text{ENR}_{\text{dB}} + 10\,\text{dB}$ noise figure [17].

$$\text{ENR} = \frac{T_{\text{hot}} - T_{\text{cold}}}{290\,\text{K}} \tag{4.1}$$

The Y-factor is the ratio of the hot and cold output power of a device when the noise source is connected at its input (Equation 4.2). The NF then calculates as in Equation 4.3.

$$Y = \frac{P_{\text{hot}}}{P_{\text{cold}}} \tag{4.2}$$

$$F = \frac{\text{ENR}}{Y - 1} \tag{4.3}$$

4.1.3.2 Measurement Setup

The Y-factor method is used to identify the NF of the receiver prototype. The required noise power measurement utilizes a spectrum analyzer (SA) in 'zero span' mode (i.e. the frequency it not swept but fixed) with an appropriate resolution bandwidth (RBW) of at most the LDACS-1 channel bandwidth ($\approx 500\,\text{kHz}$)[4]. The measurement of the receiver's noise figure is performed as follows:

1. For a calibration of the setup, the noise source is directly connected to the SA (Figure 4.6a). The 'hot' and 'cold' power levels ($P_{\text{SA}_{\text{hot}}}$ and $P_{\text{SA}_{\text{cold}}}$) of the spectrum analyzer are measured. The noise figure F_{SA} of the latter can then be calculated (Equation 4.2 and 4.3).

2. Step 1 is repeated with the receiver inserted between noise source and SA (Figure 4.6b) which gives the power levels $P_{\text{SYS}_{\text{hot}}}$ and $P_{\text{SYS}_{\text{cold}}}$ as well as the system noise figure F_{SYS}. The gain of the receiver G_{RX} can then be calculated as in Equation 4.4.

$$G_{\text{RX}} = \frac{P_{\text{SYS}_{\text{hot}}} - P_{\text{SYS}_{\text{cold}}}}{P_{\text{SA}_{\text{hot}}} - P_{\text{SA}_{\text{cold}}}} \tag{4.4}$$

3. The NF of the receiver is finally given by Equation 4.5:

[4]The RBW has to be at most the channel bandwidth because the implemented receiver's channel selection filters out-of-band noise power. This would lead to an incorrect calculation of the Y-factor.

$$F_{\mathrm{RX}} = F_{\mathrm{SYS}} - \frac{F_{\mathrm{SA}} - 1}{G_{\mathrm{RX}}} \tag{4.5}$$

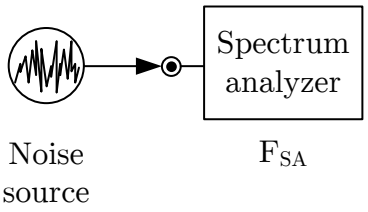

(a) Determination of the spectrum analyzers noise figure F_{SA}.

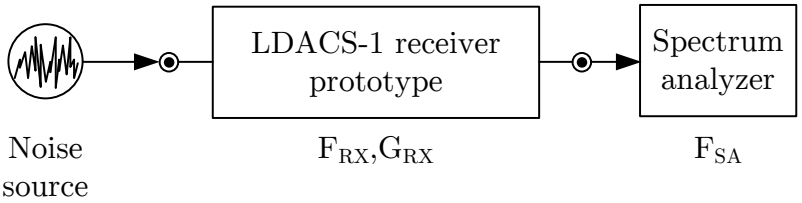

(b) RX prototype is inserted between noise source and spectrum analyzer to determine its NF and gain.

Figure 4.6: Noise figure measurement setup utilizing the hot/cold method. A spectrum analyzer in zero span mode (with an appropriate RBW) is used to measure noise powers from which the Y-factor can be calculated.

4.1.3.3 Measurement Result

The measurement was carried out using an *Agilent E4446A PSA* spectrum analyzer and a *MT7618E* noise source from *Maury Microwave Corporation*. The noise figure of the receiver prototype was determined to $\mathbf{F_{RX} \approx 3.77\,dB}$[5] which is somewhat above the calculated value from Section 3.3.1 but clearly better than the specified 5 dB.

4.1.4 Recovery Time

In case of interference power that is much higher than typical signal power, one or more components in the receiver chain are expected to saturate. The

[5]The frequency response of the receiver prototype leads to a frequency dependent in-band noise figure. The frequency dependence is mainly caused by the channel selection filters which are located after the VGA providing much gain. The influence of the frequency response onto the noise figure can, therefore, be neglected (Appendix A).

interfering signal can have a power level of up to $P_{\mathrm{DME}} = 25\,\mathrm{dBm}$ (Section 2.4.5). When it disappears, it takes a specific time t_{Recovery} till the nominal gain is re-established (Figure 4.7)—this time span is called the recovery time. The specification [6] defines this parameter by *'...shall not cause irregularities or long recovery times...'* which is not very concrete. Thus, it was appointed with *Frequentis* to have a measurable value: The receiver shall not add more than than $2\,\mu\mathrm{s}$ of blanking caused by saturation of its components. Other effects, like settling time of filters, are not considered in this context.

Figure 4.8a shows the step response at the output of the RX prototype when excited with an input signal as depicted in Figure 4.7 ($P_{\mathrm{sig}} = -70\,\mathrm{dBm}$). It takes much more than the mentioned $2\,\mu\mathrm{s}$ for the output to return to nominal gain. It shall now be investigated if this exceeds the specification or not (i.e. if it origins from saturation effects or e.g. filter settling time).

The LDACS-1 system has a channel bandwidth of approximately 500 kHz (250 kHz in equivalent baseband) which leads to a raw estimate for the filter rise/fall time of $t_r = 0.35/250\,\mathrm{kHz} = 1.4\,\mu\mathrm{s}$ [18]. The step response of the channel selection filter (Figure 4.8b) shows that these filters have an even longer settling time of about $10\,\mu\mathrm{s}$ and introduce a group delay of about $2\,\mu\mathrm{s}$, too. It is then obvious that the major part of the input/output delay (Figure 4.8a) is caused by the filters. Therefore, the specification is not necessarily exceeded as the delay isn't caused by saturation effects.
Figure 4.9 shows the step response of the receiver chain at the output of the VGA to investigate the recovery time of the amplifiers before the SAW filters. The recovery time of the chain till this stage can be observed to be **less than $1.3\,\mu\mathrm{s}$** and so clearly meets the specification.

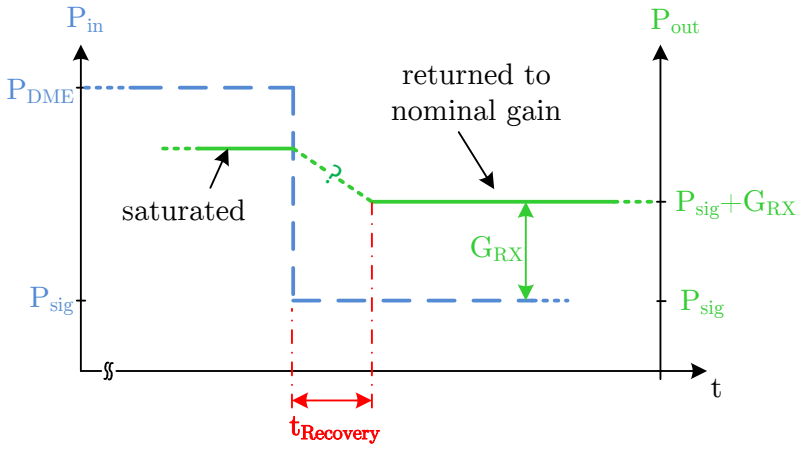

Figure 4.7: The recovery time t_{Recovery} is determined as the time the receiver needs to return to nominal gain G_{RX} after an strong interference input power of $P_{\mathrm{DME}} = 25\,\mathrm{dBm}$ (settling time of filters shall not be included).

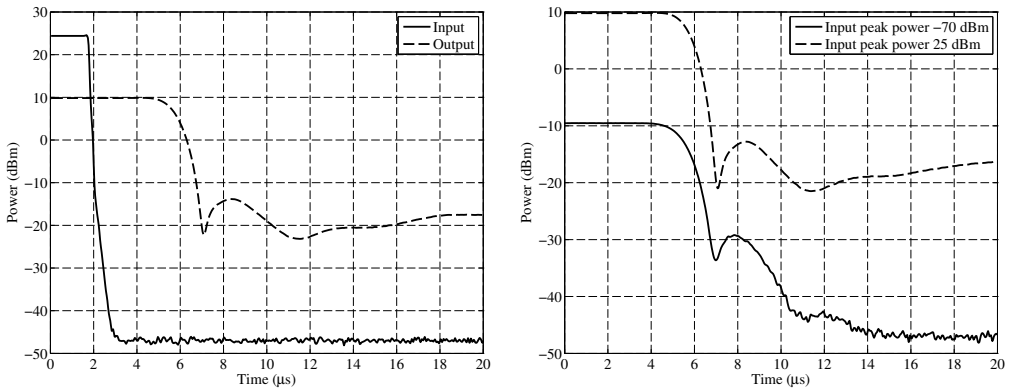

(a) RX output step response.

(b) *SAWTEK 854651* step response.

Figure 4.8: Time responses of the channel selection filters. They show about $10\,\mu\mathrm{s}$ settling time.

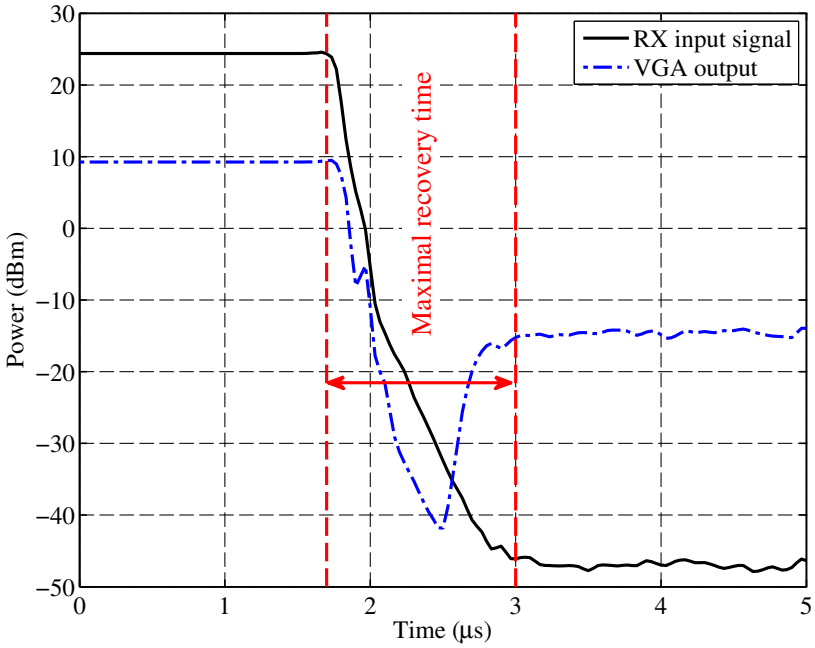

Figure 4.9: Step response of the receiver chain at the output of the VGA.

4.1.5 Frequency Response

The baseband unit needs to compensate the frequency response of the receiver in order to demodulate the OFDM symbols in a correct manner. This equalization requires attenuation and phase shift for each subcarrier.
To determine the frequency response of the RX prototype, a measurement setup as depicted in Figure 4.10 is used. A *Rohde&Schwarz SMBV100A* signal source generates an LDACS-1 signal which is passed through the receiver. It is then sampled by an *Agilent E1439C* system (containing a 95 MSPS ADC with appropriate filters and memory) and demodulated using MATLAB®. The frequency response can then be identified by comparison with the (known) input signal.
Figure 4.11 shows an I/Q-diagram of un-equalized demodulated OFDM symbols. It is observable that the receiver introduces remarkable frequency dependent attenuation and phase shift which is shown in Figure 4.12 for each subcarrier.

4.1.6 Signal to Noise Ratio

The SNR is not defined in the LDACS-1 specification but has been derived in Section 2.4.1 out of the defined Bit Error Rate in order to have an equivalent RF requirement. A minimal SNR of 4.7 dB at the output of the receiver should enable the baseband unit to accomplish the targeted BER.

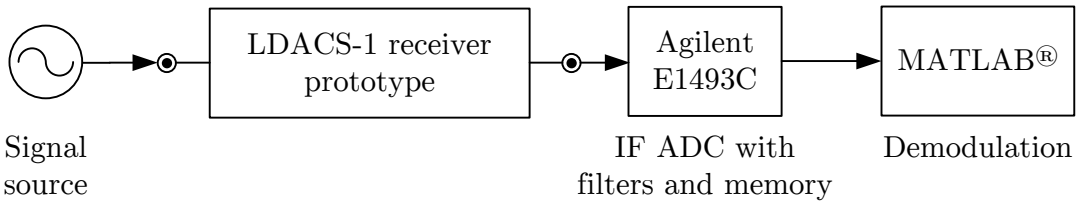

Figure 4.10: Measurement setup for the determination of frequency response and SNR.

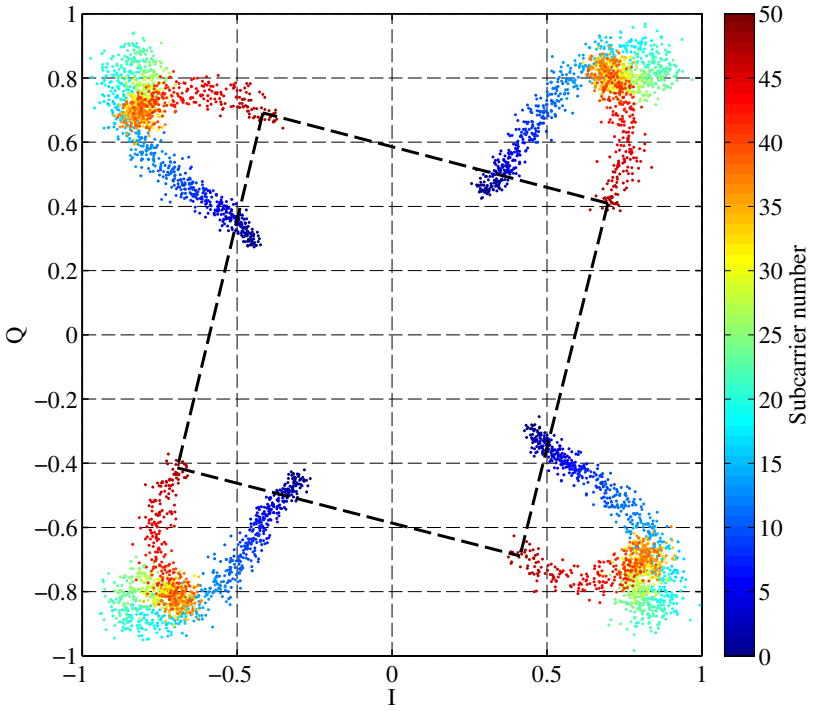

Figure 4.11: Un-equalized OFDM symbols (50 subcarriers, 100 symbols, power normalized, SNR $\approx$ 27.2 dB). The rotated constellation is shown exemplary for the 50^{th} subcarrier.

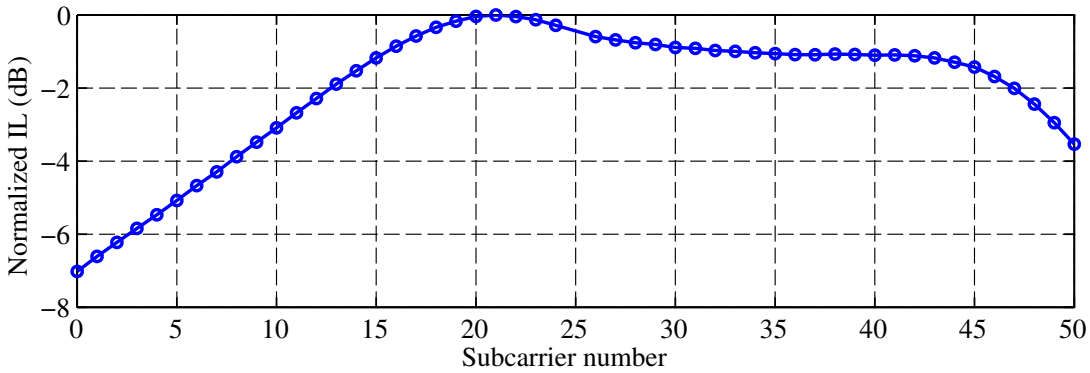

(a) Normalized insertion loss

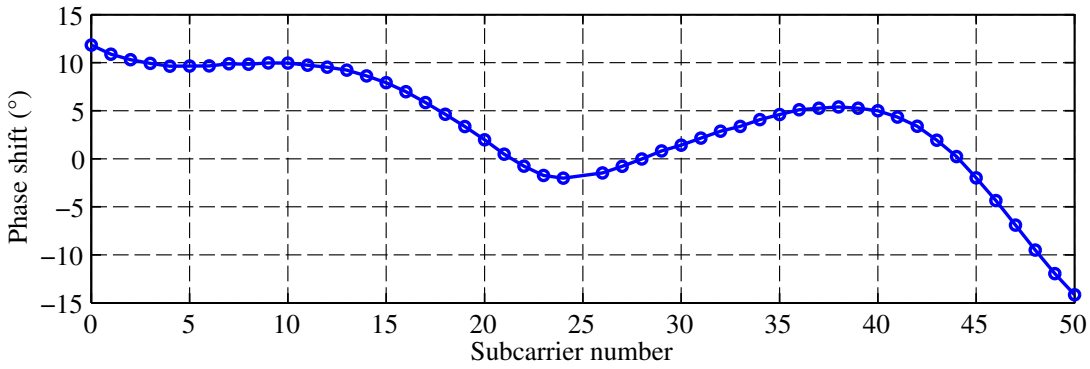

(b) Phase shift

Figure 4.12: Subcarrier dependent attenuation and phase shift. DC subcarrier (No.25) omitted.

The corresponding measurement can be realized with the same setup as for the frequency response (Figure 4.10) with an LDACS-1 signal at a power level of $P_{\text{in}} = -104\,\text{dBm}$. In order to determine the SNR, the recorded signal (from the ADC) has to be equalized utilizing the frequency response found in Section 4.1.5. The resulting **SNR is calculated to 8.27 dB** which fits quite well to the calculated value of 8 dB (Section 2.4.1) and so fulfills the requirements. Figure 4.13 illustrates the corresponding demodulated and equalized OFDM symbols in an I/Q-diagram.

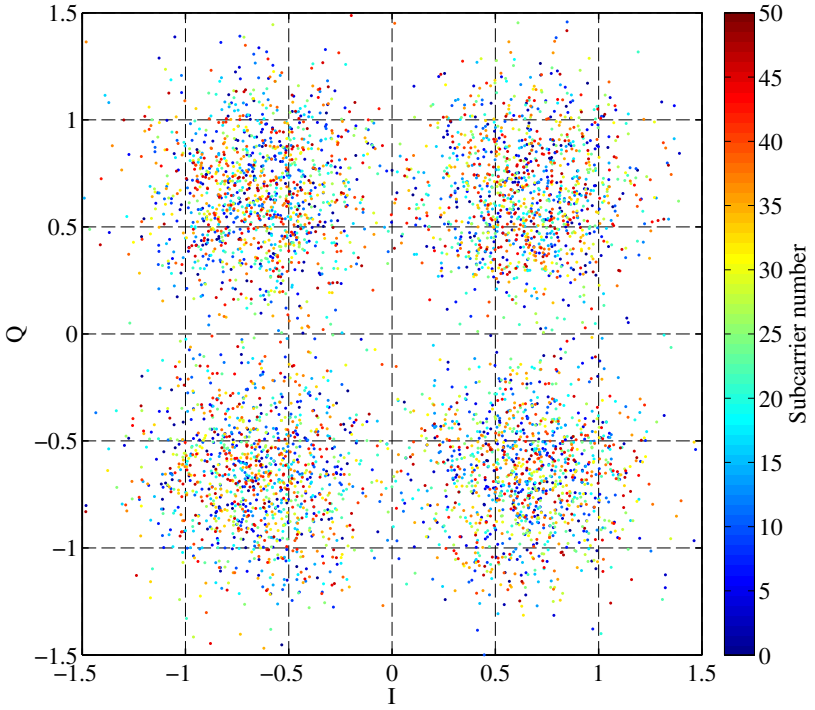

Figure 4.13: 100 equalized and demodulated OFDM symbols at the output of the receiver (50 subcarriers, power normalized, input signal level $P_{\text{in}} = -104\,\text{dBm}$, maximal VGA gain). The SNR is determined to about 8.27 dB.

4.2 Summary

This chapter showed measurements of a practical implementation of an LDACS-1 receiver. The according values and measurement setups for meeting the standard were presented which showed that the prototype presented in this thesis fulfills or surpasses all requirements. Furthermore, the frequency response of the receiver (for each OFDM subcarrier) was presented which can be used for the baseband unit to perform equalization. Table 4.1 summarizes the required and achieved performance parameters.

Parameter	**Required**	**Achieved**	**Unit**
Frequency range	$960 \ldots 1164$	✓	MHz
Channel bandwidth	0.5	✓	MHz
Input signal power	$-104 \ldots -10$	✓	dBm
Noise figure	≤ 5	3.77	dB
Gain (967 MHz)	$21 \ldots 47$	$6.7 \ldots 52.4$	dB
Gain (1163 MHz)	$21 \ldots 47$	$10.2 \ldots 55.5$	dB
IF gain variation	–	$-5/2$	dB
P1dB	≥ -10	-9.5	dBm
Abs. max. input power	≥ 25	27	dBm
Recovery time (after interference pulse)	≤ 2	≤ 1.3	μs

Table 4.1: Summarized requirements and measurements for the RX prototype.

Chapter 5

Summary and Outlook

This chapter presents a short summary as well as further development options for the the implemented receiver.

5.1 Summary

In this thesis the RF frontend of an LDACS-1 compliant receiver was designed, built, and measured in order to verify the compliance with the standard. The frontend was designed to operate in the frequency range of $960 \ldots 1164\,\mathrm{MHz}$ for input signal power level of $-104 \ldots -10\,\mathrm{dBm}$, providing enough SNR at its output to enable the baseband unit to achieve the targeted BER of less than 10^{-6}. The maximal input power handling of up to $25\,\mathrm{dBm}$ was verified in order to withstand DME pulses.

5.2 Outlook

The receiver PCB was designed in order to allow the future implementation of features which are beyond the scope of this thesis:

- **Automatic Gain Control (AGC)**
  The voltage for the VGA of the prototype presented in this thesis is supposed to be externally controlled by the baseband unit in order to set an appropriate gain for the input signal power. To allow the autonomous operation of the frontend, a power detector after the VGA can be utilized to provide a signal which is proportional to the actual power level. This can be used to generate a control signal for the VGA (Figure 5.1).

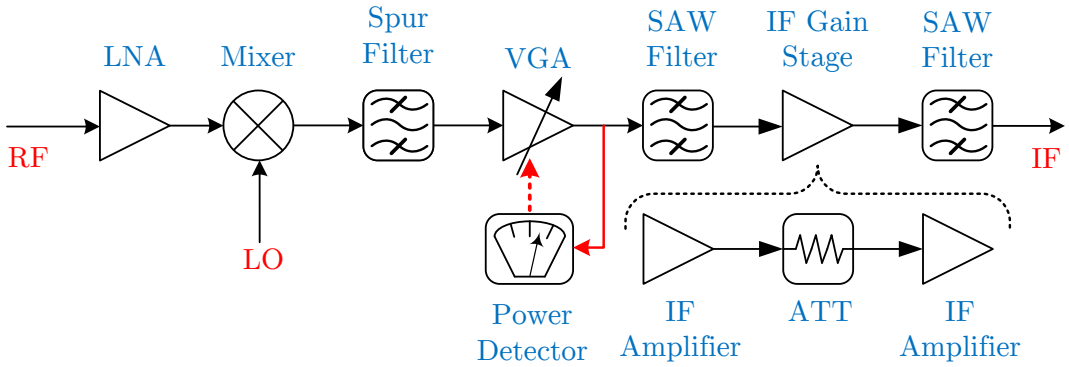

Figure 5.1: A power detector after the VGA can be used in order to implement an autonomous AGC.

- **Power detector for DME pulse detection**
  The LDACS-1 standard foresees the use of pulse blanking and erasure decoding. To accomplish this, the baseband unit needs the RX frontend to provide a fast detection of interfering signals. A possible realization is the introduction of a power detector right at the input of the receiver combined with a fast comparator as depicted in Figure 5.2.

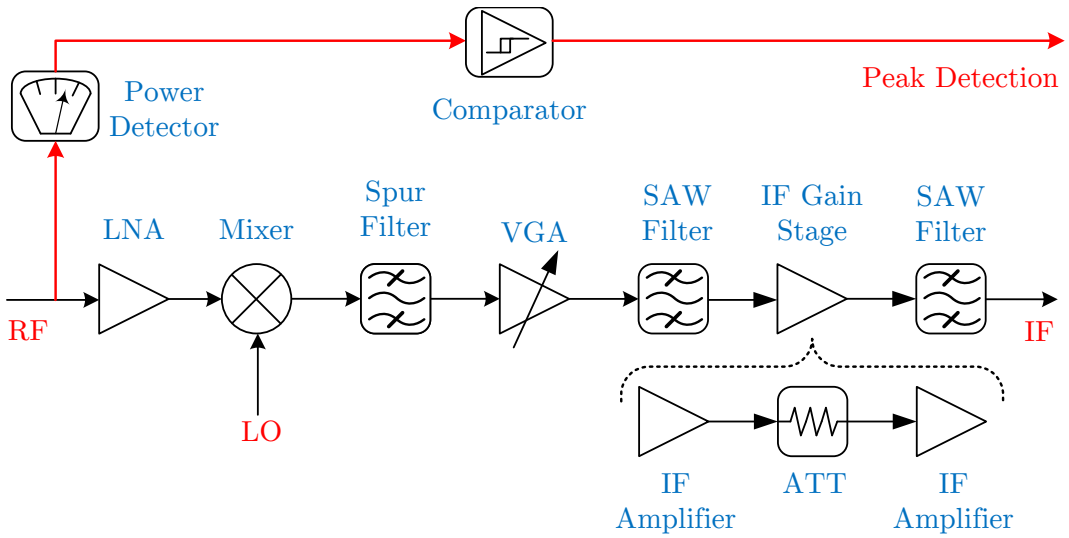

Figure 5.2: A power detector at the input can be used in order provide peak power detection to the baseband unit.

References

[1] Eurocontrol, "Long-Term Forecast IFR Flight Movements 2010-2030," 2010.

[2] Austro Control GmbH, "Enroute Chart – ICAO (Lower Airspace)," 09 2012.

[3] M. Sajatovic and M. Schnell, "Updated LDACS1 Prototype Specification," Tech. Rep. EWA04-1-T2-D2, Frequentis AG / DLR, 02 2004.

[4] J. Micallef, R. Womersley, S. Dunkley, and I. Casewell, "L-band interference scenarios characterisation," tech. rep., Eurocontrol, 08 2009.

[5] Deutsches Zentrum für Luft- und Raumfahrt e.V. (DLR), "Proposed L-Band Interference Scenarios," 02 2008.

[6] M. Sajatovic, B. Haindl, C. Rihacek, M. Schnell, S. Gligorevic, and S. Brandes, "L-DACS1 System Definition Proposal: Deliverable D3 - Design Specification for L-DACS1 Prototype," Tech. Rep. 1.0, Deutsches Zentrum für Luft- und Raumfahrt e.V. (DLR), 04 2009.

[7] Analog Devices, Inc., "Datasheet of 16-Bit, 170/200-MSPS Analog-to-Digital Converter," 10 2009.

[8] RF Micro Devices, Inc., "Datasheet of SPF-5189Z - 50MHz to 4000MHz, GaAs pHEMT Low Noise MMIC Amplifier," 2006.

[9] Hittite Microwave Corporation, "Datasheet of HMC686LP4 - BiCMOS Mixer with Integrated LO Amplifier, 700-1500 MHz," 05 2009.

[10] TriQuint Semiconductor, "Datasheet of SAWTEK 854651 SAW Filter," 11 1999.

[11] Analog Devices, Inc., "Datasheet of AD8367 - 500 MHz, Linear-in-dB VGA with AGC Detector," 2005.

[12] Mini Circuits, "Datasheet of SXBP-70+ Surface Mount Bandpass Filter."

[13] Mini Circuits, "Datasheet of LFCN-1200 Ceramic Low Pass Filter," 2007.

[14] Mini Circuits, "Datasheet of LFCN-3000 Ceramic Low Pass Filter," 2007.

[15] Analog Devices, Inc., "Datasheet of ADL5535 - 20 MHz to 1.0 GHz IF Gain Block," 2010.

[16] Analog Devices, Inc., "Datasheet of ADL5536 - 20 MHz to 1.0 GHz IF Gain Block," 2010.

[17] Agilent Technologies, "Fundamentals of RF and Microwave Noise Figure Measurements," 2010.

[18] C. Mittermayer and A. Steininger, eds., *On the Determination of Dynamic Errors for Rise Time Measurement with an Oscilloscope*, vol. 48 of *IEEE Transactions on Instrumentation and Measurement*, IEEE, 1999.

Appendices

Appendix A

Noise Figure Calculation

Component	**Parameter**	**Value (dB)**
SPF-5189z	F_{LNA}	0.79
	G_{LNA}	$\underline{16.8} \ldots 18.2$
HMC686LP4	F_{Mixer}	10.5
	G_{Mixer}	-7.5
SpurFilter	F_{SF}	1.1
	G_{SF}	-1.1
AD8367	F_{VGA}	$\underline{7.5} \ldots 52.5$
	G_{VGA}	$-2.5 \ldots \underline{42.5}$
854651	F_{SAW}	$7.6 \ldots \underline{10.87}$
	G_{SAW}	$-7.6 \ldots \text{-}\underline{10.87}$
ADL5536	F_{IFAmp1}	2.4
	G_{IFAmp1}	20
ATT	F_{ATT}	10
	G_{ATT}	-10
ADL5535	F_{IFAmp2}	3
	G_{IFAmp2}	16.5

Table A.1: Summarized component parameters. For the parameters having a range the underlined value was used for noise figure calculation.

$$
\begin{aligned}
F_{Chain} = & \underbrace{F_{LNA}}_{1.1995} + \underbrace{\frac{F_{Mixer}-1}{G_{LNA}}}_{0.2135} + \underbrace{\frac{F_{SF}-1}{G_{LNA}\cdot G_{Mixer}}}_{0.033518} + \underbrace{\frac{F_{VGA}-1}{G_{LNA}\cdot G_{Mixer}\cdot G_{SF}}}_{0.69817} \\
& + \underbrace{\frac{F_{SAW1}-1}{G_{LNA}\cdot G_{Mixer}\cdot G_{SF}\cdot G_{VGA}}}_{95.261\cdot 10^{-6}} + \underbrace{\frac{F_{IFAmp1}-1}{G_{LNA}\cdot G_{Mixer}\cdot G_{SF}\cdot G_{VGA}\cdot G_{SAW1}}}_{76.721\cdot 10^{-6}} \\
& + \underbrace{\frac{F_{ATT}-1}{G_{LNA}\cdot G_{Mixer}\cdot G_{SF}\cdot G_{VGA}\cdot G_{SAW1}\cdot G_{IFAmp1}}}_{91.457\cdot 10^{-6}} \\
& + \underbrace{\frac{F_{IFAmp2}-1}{G_{LNA}\cdot G_{Mixer}\cdot G_{SF}\cdot G_{VGA}\cdot G_{SAW1}\cdot G_{IFAmp1}\cdot G_{ATT}}}_{10.114\cdot 10^{-6}} \\
& + \underbrace{\frac{F_{SAW2}-1}{G_{LNA}\cdot G_{Mixer}\cdot G_{SF}\cdot G_{VGA}\cdot G_{SAW1}\cdot G_{IFAmp1}\cdot G_{ATT}\cdot G_{IFAmp2}}}_{2.552\cdot 10^{-6}} \\
= & \, 2.1469 \approx \mathbf{3.32\,dB}
\end{aligned}
\tag{A.1}
$$